AD-A089 827 ROCKWELL INTERNATIONAL THOUSAND OAKS CA SCIENCE CENTER F/G 11/6
MECHANISMS BY WHICH HUMIDITY ALTERS DUCTILITY.(U)
AUG 80 W L MORRIS, M R JAMES, O BUCK, R CHANG N00014-79-C-0334
UNCLASSIFIED SC5211.1TR NL

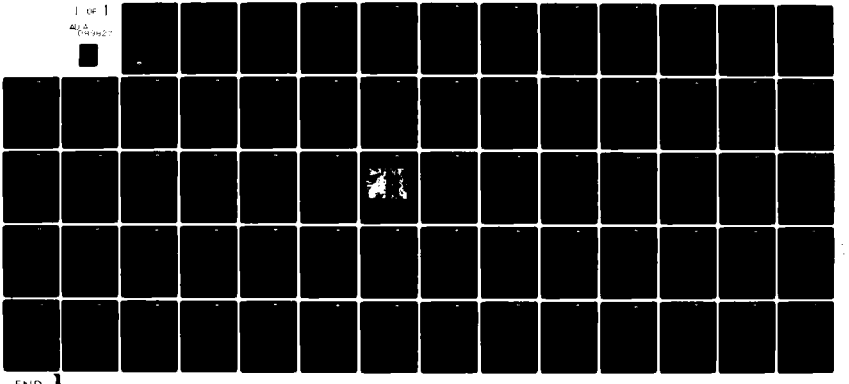

END
DATE FILMED
11-80
DTIC

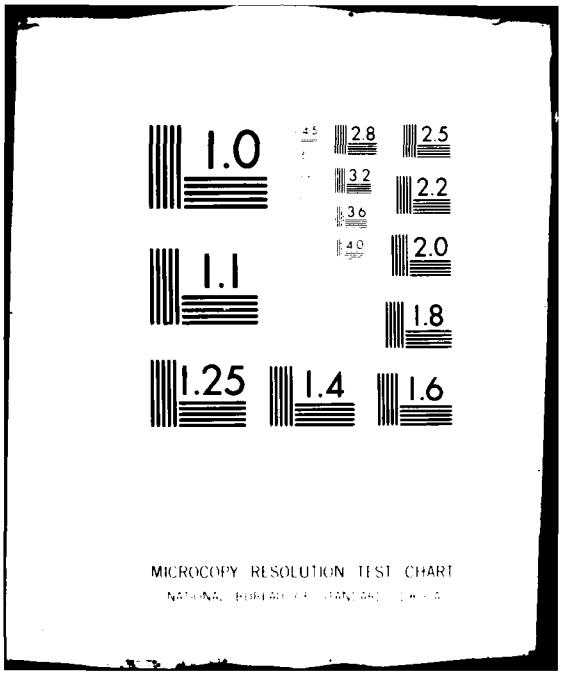
1.0
2.8
2.5
3.2
2.2
3.6
4.0
2.0
1.1
1.8
1.25
1.4
1.6
MICROCOPY RESOLUTION TEST CHART

LEVEL II

SC5211.1TR

Copy No. 1

SC5211.1TR

MECHANISMS BY WHICH HUMIDITY ALTERS DUCTILITY

TECHNICAL REPORT FOR THE PERIOD
April 15, 1979 through April 14, 1980

AD A089827

GENERAL ORDER NO. 5211
CONTRACT NO. N00014-79-C-0334

Prepared for

Office of Naval Research
Department of the Navy
800 N. Quincy Street
Arlington, VA 22217

W. L. Morris
Principal Investigator

AUGUST 1980

Research was sponsored by the Office of Naval Research under contract number N00014-79-C-0334, project number NR 036-134 (471).

Rockwell International
Science Center

UNCLASSIFIED

SECURITY CLASSIFICATION OF THIS PAGE (When Data Entered)

REPORT DOCUMENTATION PAGE	READ INSTRUCTIONS BEFORE COMPLETING FORM
1. REPORT NUMBER	2. GOVT ACCESSION NO. AD-A089 827 / 3. RECIPIENT'S CATALOG NUMBER
4. TITLE (and Subtitle) (6) Mechanisms By Which Humidity Alters Ductility.	5. TYPE OF REPORT & PERIOD COVERED Technical Report for period 04/15/79 through 4/14/80
	6. PERFORMING ORG. REPORT NUMBER (14) SC5211.1TR
7. AUTHOR(s) (10) W. L. Morris, M. R. James, O. Buck, R. Chang, J. W. Wert	8. CONTRACT OR GRANT NUMBER(s) N00014-79-C-0334
9. PERFORMING ORGANIZATION NAME AND ADDRESS Rockwell International Science Center 1049 Camino Dos Rios Thousand Oaks, CA 91360	10. PROGRAM ELEMENT, PROJECT, TASK AREA & WORK UNIT NUMBERS NR 036-134 (471)
11. CONTROLLING OFFICE NAME AND ADDRESS Office of Naval Research, Dept. of the Navy 800 N. Quincy Street Arlington, VA 22217	12. REPORT DATE (11) August 1980
	13. NUMBER OF PAGES 68
14. MONITORING AGENCY NAME & ADDRESS (if different from Controlling Office)	15. SECURITY CLASS. (of this report) Unclassified
	15a. DECLASSIFICATION/DOWNGRADING SCHEDULE

16. DISTRIBUTION STATEMENT (of this Report)

Approved for public release; distribution unlimited

17. DISTRIBUTION STATEMENT (of the abstract entered in Block 20, if different from Report)

18. SUPPLEMENTARY NOTES

19. KEY WORDS (Continue on reverse side if necessary and identify by block number)

ductility, surface properties, corrosion environments, fatigue, cracking, fatigue properties, surface defects, crack initiation, aluminum alloys, plastic theory

20. ABSTRACT (Continue on reverse side if necessary and identify by block number)

The mechanical properties of a thin layer at the surface of aluminum alloys change progressively during fatigue. The alterations are more pronounced and rapid for fatigue in moist than in dry air. ~~We characterize the alterations~~ WAS CHARACTERIZED, observed as a change in the 'ductility' of the surface, and ~~find that~~ THE rates of crack initiation, early growth and the relaxation of residual surface stresses during fatigue are all sensitive to the state of ductility of the surface, WAS FOUND. The depth into the surface affected by environment is too shallow – (cont'd)

DD FORM 1 JAN 73 1473 EDITION OF 1 NOV 65 IS OBSOLETE

UNCLASSIFIED

SECURITY CLASSIFICATION OF THIS PAGE When Data Entered

#20 ABSTRACT

to permit characterization of the surface ductility by conventional techniques. We describe the development, evaluation and refinement of procedures to determine the ductility of the surface during fatigue; which rely upon characterization of the microplasticity of the surface, in plastic zones at the tips of short surface cracks. A study of the fundamental mechanisms underlying deformation at crack tips allows us to compensate for the effect which crack length and grain size has on the microscopic deformation, and we thus obtain fundamental ductility parameters which are relatable to alloy type, composition, heat treatment and humidity. Five parameters, related to different aspects of surface ductility, are defined and methods to measure them are discussed. Results of an initial survey of the relationship of alloy type and heat treatment to the sensitivity of surface ductility to humidity are also described.

TABLE OF CONTENTS

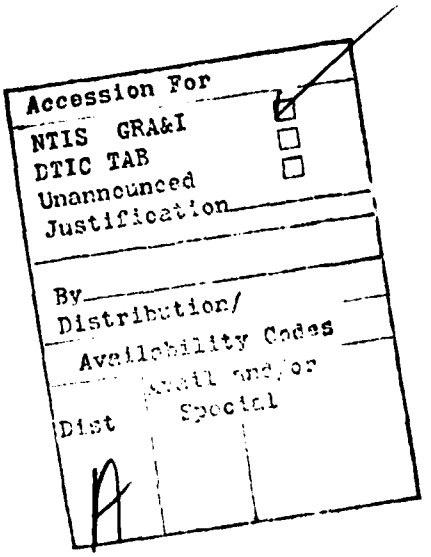

LIST OF FIGURES

LIST OF FIGURES

ABSTRACT

The mechanical properties of a thin layer at the surface of aluminum alloys change progressively during fatigue. The alterations are more pronounced and rapid for fatigue in moist than in dry air. We characterize the alterations observed as a change in the "ductility" of the surface, and find that rates of crack initiation, early growth and the relaxation of residual surface stresses during fatigue are all sensitive to the state of ductility of the surface. The depth into the surface affected by environment is too shallow to permit characterization of the surface ductility by conventional techniques. We describe the development, evaluation and refinement of procedures to determine the ductility of the surface during fatigue; which rely upon characterization of the microplasticity of the surface, in plastic zones at the tips of short surface cracks. A study of the fundamental mechanisms underlying deformation at crack tips allows us to compensate for the effect which crack length and grain size has on the microscopic deformation, and we thus obtain fundamental ductility parameters which are relatable to alloy type, composition, heat treatment and humidity. Five parameters, related to different aspects of surface ductility, are defined and methods to measure them are discussed. Results of an initial survey of the relationship of alloy type and heat treatment to the sensitivity of surface ductility to humidity are also described.

1.0 NOMENCLATURE

c	Halfcrack length
CTOD	Crack tip opening displacement, measured at a tip at the surface
$CTOD_p$	The plastic component of CTOD
D	Grain size
N	Number of fatigue cycles
N_S	Number of fatigue cycles at onset of incubation
S	Effective maximum surface stress
z_o	Distance of crack tip to grain boundary
β	Material parameter related to critical strain energy density required for propagation
$\delta(\sigma_{max})$	Opening at crack center at stress, σ_{max}
ΔK_{eff}	Effective stress intensity range
ΔN_I	Number of cycles required for incubation
ε_y	Strain in the plastic zone
ε'_y	Normalized strain parameter proportional to ε_y
ξ	Material parameter describing rate of increase in strain in the plastic zone
τ	Surface shear stress
τ_f	Surface shear stress at the fatigue limit
τ_i	Friction shear stress on cyclically harden surface
τ_o	Minimum surface shear stress producing microplastic deformation
σ_{max}	Maximum tensile stress amplitude
σ_{yield}	Alloy yield strength
θ	Coefficient of cyclic hardening.

2.0 INTRODUCTION

Environmental humidity substantially affects the rate at which cracks initiate and grow on the surface of aluminum alloys during fatigue.[1,2] It appears that the principal effect of humidity is to decrease the ductility of the alloy surface.[3] The sensitivity of aluminum alloys to humidity varies with alloy type, with heat treatment and apparently with minor changes in the chemical composition of an alloy. The goal of this research is to model the synergistic effects of these material parameters with humidity to predict surface ductility and hence fatigue behavior. It is hoped that one ultimate application of such results will be to suggest alloy compositional and heat treatment regimes which will be least sensitive to fatigue damage.

Everyone has a concept of the meaning of ductility. Ductility as typically encountered in metallurgy is not a fundamental quantity however, but is definable only in terms of the procedure used to measure it. A reduction in area test simultaneously assesses the contribution from several factors which affect the amount of deformation a material will sustain before failure. These include hardenability, and resistance to crack initiation and to crack growth.

The purpose of the first year's effort in this program was to develop and evaluate procedures to characterize the ductility of the surface of aluminum alloys subjected to fatigue. Furthermore the plan was to begin a survey of the effect of alloy heat treatment, composition and humidity on properties of ductility using the new experimental techniques. Our intention

is to define a set of measurements which characterize surface ductility in as fundamental a way as possible, by defining procedures to measure individual aspects of the microplastic deformation properties of a surface.

Early growth of short surface cracks involves non-continuum processes of plastic deformation at the surface.[3] The plastic zone size of short cracks in aluminum alloys is essentially determined by the distance of the crack tip to the next grain boundary, provided that the applied stress is kept below the alloy yield strength. Slip into a new grain only begins when a surface crack tip approaches a grain boundary. Our measurements of "ductility" rely upon determination of the rate at which the plastic zone develops in the new grain during fatigue; and upon determination of the equilibrium value of the plastic component of opening displacement of the surface crack tip, when growth into the new grain begins after the plastic zone is mature.

Interpretation of such measurements requires a fundamental understanding of microscopic processes involved in early crack growth. Our discoveries in the past year regarding growth mechanisms, their relationship to ductility and an initial survey of the ductility of selected alloys are discussed in Section 4.0. The role of the ductility parameters, we define, in crack initiation and in relaxation of residual surface stresses during fatigue is discussed in Section 5.0.

3.0 EXPERIMENTAL PROCEDURES

Early crack growth measurements are made using miniature flexural fatigue specimens, tapered to achieve a uniform surface stress over the specimen gauge section. The detailed specimen geometry has been reported elsewhere.[2] Specimens are prepared by machining with progressively shallower cutting depths to minimize residual surface stress. Final cutting depth is approximately 20 μm and thereafter specimens are mechanically polished ending with a 0.05 μm alumina powder. Residual surface stresses obtained with this procedure, and measured by x-ray diffraction, are small (<20 MN/m^2).

Specimens are fatigued in laboratory air (humidity measured) and are loaded in stroke control with the loading fully reversed ($R = \sigma_{min}/\sigma_{max} = -1$) at approximately 5 Hz. They are then transferred at intervals to either a scanning electron or optical microscope to measure the crack tip deformation or growth parameters of interest.

A dry box has been constructed which can be used to maintain the specimen in a dry air environment. This is flushed for several hours with dry air, and then a cold (liquid nitrogen cooled) probe is exposed to pump any residual moisture. We have found the system workable but cumbersome and time consuming to use. To replace it, we have evaluated the use of surface coatings which could prevent penetration of ambient moisture to the surface during fatigue. Lacomit, which is a commercially available stop coating material used in electropolishing, was found to provide the desired characteristics. We find the fatigue crack initiation and early growth behavior in dry air and

with specimens coated with Lacomit to be the same. By coating one side of a specimen with Lacomit and leaving the other exposed to ambient humidity, the effect of humidity can be evaluated on a single specimen.

4.0 DUCTILITY MEASUREMENTS

Short crack growth in aluminum alloys is quite discontinuous. Grain boundaries can substantially impede propagation and it is not unusual for short cracks to be completely stopped by boundaries over the entire lifetime of a fatigue specimen. The rate at which cracking proceeds across boundaries is sensitive to the ductility of the surface, and so the measurement of appropriate parameters associated with crack growth can be used to characterize ductility. In the past year we have learned that it requires five parameters to specify various aspects of surface ductility. In an analogy to bulk measurements these can be thought of as: (1) the cyclic hardenability of the surface; (2 and 3) two parameters describing the micro-plasticity of the surface below the yield strength, a magnitude per increment strain and a lower bound friction stress; and (4 and 5) and two parameters related to the ultimate material strength. It appears that the depth below the surface to which the ductility parameters can be altered by humidity is quite shallow, less than a few micrometers. Thus conventional procedures can not be used to measure the parameters of interest. [An attempt was made to use Knoop indentation hardness to assess the change of surface ductility of Al 2219-T851 with fatigue in humidity vs in dry air with negative results]. While the data are incomplete, it also appears likely that three of the parameters are sensitive to humidity as well as to the material variables. Combinations of the same parameters are required to describe the processes of crack initiation and the relaxation of residual surface stresses in aluminum alloys, as well as the

growth behavior from which they are obtained. Discussed below are the techniques used to measure the ductility parameters, the mechanisms that underlie the behavior characterized and the status of our survey of the effect of humidity and alloy type on surface ductility.

4.1 History of Crack Growth Modeling at the Science Center

We have been involved for several years in learning how to measure the closure stresses at the tips of small surface cracks. This ultimately led to the development of an empirical procedure to estimate the closure stress at a surface crack tip by measuring the opening displacement (CTOD) at the maximum tensile cyclic stress applied during fatigue.[3] As a surface crack tip enters a new grain, a closure stress develops with a magnitude proportional to the size of the grain. Closure stresses were found to be smaller for alloys fatigued in moist than in dry air, and were found to vary from alloy to alloy for a fixed grain size. It was shown, by comparing predicted and measured rates of short crack growth in Al 2219-T851, that closure stress was a substantial factor in early crack growth.[4,5] The initial concept upon writing the proposal for the present contract was to use CTOD measurement to determine surface ductility variations with humidity and with alloy type. Less surface ductility is associated with smaller values of CTOD and hence with small closure stresses.

In 1979 a series of experiments were done under the support of Rockwell IR&D funds with the aim of predicting early growth rates from the size and shape of grains in the crack path. Grain shape parameters were used

to calculate the closure stress at a crack tip at the surface, giving a predicted rate of growth based upon a ΔK_{eff} model.[4] The experiments were done using Al 2219-T851 with a cyclic stress amplitude of $\pm 0.9\ \sigma_{yield}$. We found that variations in closure stress with location of crack tips with respect to grain boundaries were sufficient to describe the majority of the growth rate observations, with one exception. Propagation rates slow down just before growth begins into a new grain, as slip commences across the boundary. We found that the retardation in growth rate was larger than predicted from the closure model if a crack tip encountered a small grain, and that with sufficiently small fatigue increments one could see that propagation actually stopped.[6]

In 1978 Chang et al[7] had proposed a model of early crack growth which considered the dynamics of development, during fatigue, of a plastic zone at a crack tip in an initially undeformed medium. It was hypothesized that development of a mature plastic zone required accumulated microplastic deformation, and it was shown that in this case crack growth would be arrested until a critical strain energy density was developed at a crack tip. The theory was first used to model the duration of non-propagation from intermetallic particles fractured during fatigue of Al 2219-T851, and successfully predicted observed statistical variations in non-growth periods with particle size and with encompassing grain size.[8]

It was realized that the Chang model had the type of dependence upon slip distance required to explain the inaccuracy of our short crack growth model. The applicability of the Chang model to crack growth into a new grain

was easily rationalized, as we knew that slip into the new grain did not occur until just before a crack tip entered a new grain.[3] Thus growth across a boundary begins essentially into an undeformed medium. We refer to the process during which the plastic zone develops as incubation. It was found that a refurbished model, incorporating the effects of grain size and shape on both closure stress and incubation period, was quite adequate to predict our experimental growth observations.[4,6]

At this point it was quite clear that the static model of CTOD behavior upon which our closure stress predictions were based was too simplistic. Fortunately, owing to its strong dependence on cyclic stress amplitude, incubation was only of secondary importance to crack growth for the large amplitudes used in the growth experiments ($\pm 0.9\ \sigma_{yield}$) allowing the effect of closure stress to be independently assessed. We expected incubation could be the dominant factor in controlling retardation of short crack growth across grain boundaries for low cyclic stress amplitude, and that the extension of the duration of the incubation period at low stress amplitude would allow us to assess the dynamics of the microplasticity at a surface crack tip.

At about the same time a new aspect of the effect of humidity on surface ductility was discovered. An ongoing project supported by Rockwell has been directed at refining and testing a model (initially developed under ONR Contract No. 00014-76-C-0452) of fatigue crack initiation at constituent surface particles. We found that particles were more easily fractured by fatigue in dry than in moist air, and furthermore that our simple particle

fracture model substantially overestimated the numbers of particles actually broken at low cyclic stress amplitudes, particularly later in the fatigue lifetime. A new initiation model was proposed in which we assumed that the friction stress (the minimum shear stress required for microplastic deformation) increased progressively during fatigue, at a rate sensitive to the environmental humidity. A simple model of the process was found adequate to explain our experimental observations.[6]

It was recognized that such cyclic hardening of the surface must also effect the incubation mechanism by altering the rate of slip into a new grain. The incubation, cyclic hardening and closure stress phenomena are sensitive to different aspects of the ductility of an alloy surface. The major thrust of our research on this contract in the past year has been directed at modeling these processes, and in definition of procedures to extract meaningful ductility parameters from such measurements. The major results of our research in the past year are as follows.

1. The physical reality of incubation has been demonstrated by measuring the progressive increase in the plastic component of CTOD ($CTOD_p$) for crack tips arrested at grain boundaries.

2. We find that cyclic hardening of the surface increases the duration of incubation by suppressing slip into a new grain.

3. A model of the incubation period has been constructed which considers the effect of grain size, crack length, cyclic hardening, grain crystallographic orientation and stress amplitude on the incubation period. Predictions of several aspects of this model have been tested and the model appears to be good.

4. A model of the effect of constraint of slip by grain boundaries on closure stress has been developed, whose predictions agree with our empirical closure stress equations. A simplified model of the progressive increase of $CTOD_p$ during incubation has also been devised and appears adequate to explain our observations.

5. A set of five parameters describing surface ductility and procedures to measure these parameters have been defined.

6. An initial survey of the effect of heat treatment and humidity on surface ductility is complete.

4.2 Equilibrium Growth Phenomena

Rice[9] has suggested that the plastic component of crack tip opening displacement $CTOD_p \approx \varepsilon_y z_o/2$, where z_o is the size of the plastic zone and ε_y is the strain at the yield strength. For short surface cracks in aluminum alloys fatigued below the yield strength, z_o is the distance of the crack tip

to the next grain boundary.[3] A measurement of $CTOD_p$ vs z_o can therefore be used to obtain ε_y, a parameter which describes one facet of ductility. Results typical for Al 2219-T851 alloy are shown in Fig. 1. Parameters of short surface cracks are measured in the SEM using a jig which permits specimens to be loaded to the maximum tensile stress applied during fatigue (Fig. 2). Measurements made for each crack tip are illustrated in Fig. 3. We infer from results of an analysis by Green and Sneedon[10] that for an elastic crack (i.e., as $z_o \to 0$) $CTOD/\delta(\sigma_{max}) \approx 0.1$. The parameter $\delta(\sigma_{max})$ is the opening at the center of the crack and is approximately proportional to the crack length 2c. Thus with the normalization used in Fig. 1, all deformation above the dashed line is plastic. For convenience, we define a normalized strain ε_y' given by Eq. (1), which represents a normalized failure strain for the material in environment. The actual strain $\varepsilon_y \approx 0.0182\ \sigma_{max}\varepsilon_y'/\sigma_{yield}$. The proportionalty coefficient comes from the ratio of crack opening to crack length, which is only approximately known. Thus ε_y' is determinable with more accuracy than is ε_y.

$$\varepsilon_y' = \frac{2c}{z_o}\left[\frac{CTOD}{\delta(\sigma_{max})} - 0.1\right] \qquad (1)$$

Values of ε_y' measured in this manner for alloys Al 2219-T851 and Al 7075-T6 are listed in Appendix A. Attempts to measure ε_y' for Al 2024-T3 yielded the erroneous result, $\varepsilon_y' = 0$. This is an artifact of the measurement procedure which arises when the cracks in the data set are crystallographic. Apparently the plastic deformation associated with the growth of

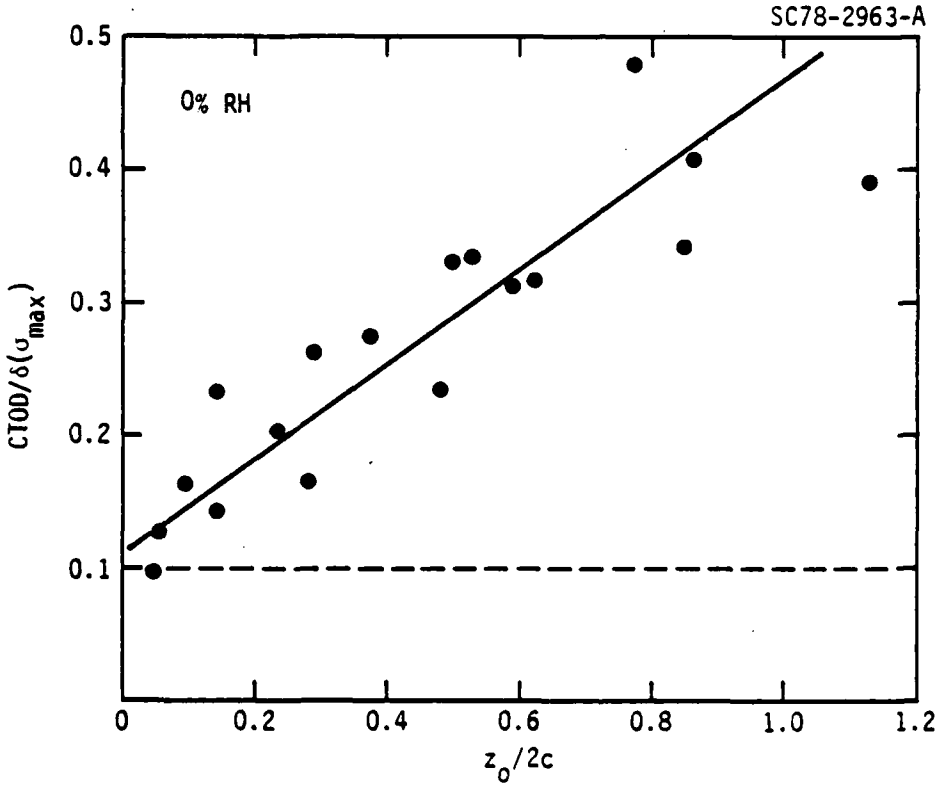

Fig. 1 Crack tip opening displacement vs distance z_0 of the crack tip to the next grain boundary for Al 2219-T851. With the normalization used a value of $CTOD/\delta(\sigma_{max}) = 0.1$ is the elastic component of the opening displacement. Plastic component increases with increased distance of crack tip to boundary. Dashed line is predicted elastic opening displacement.

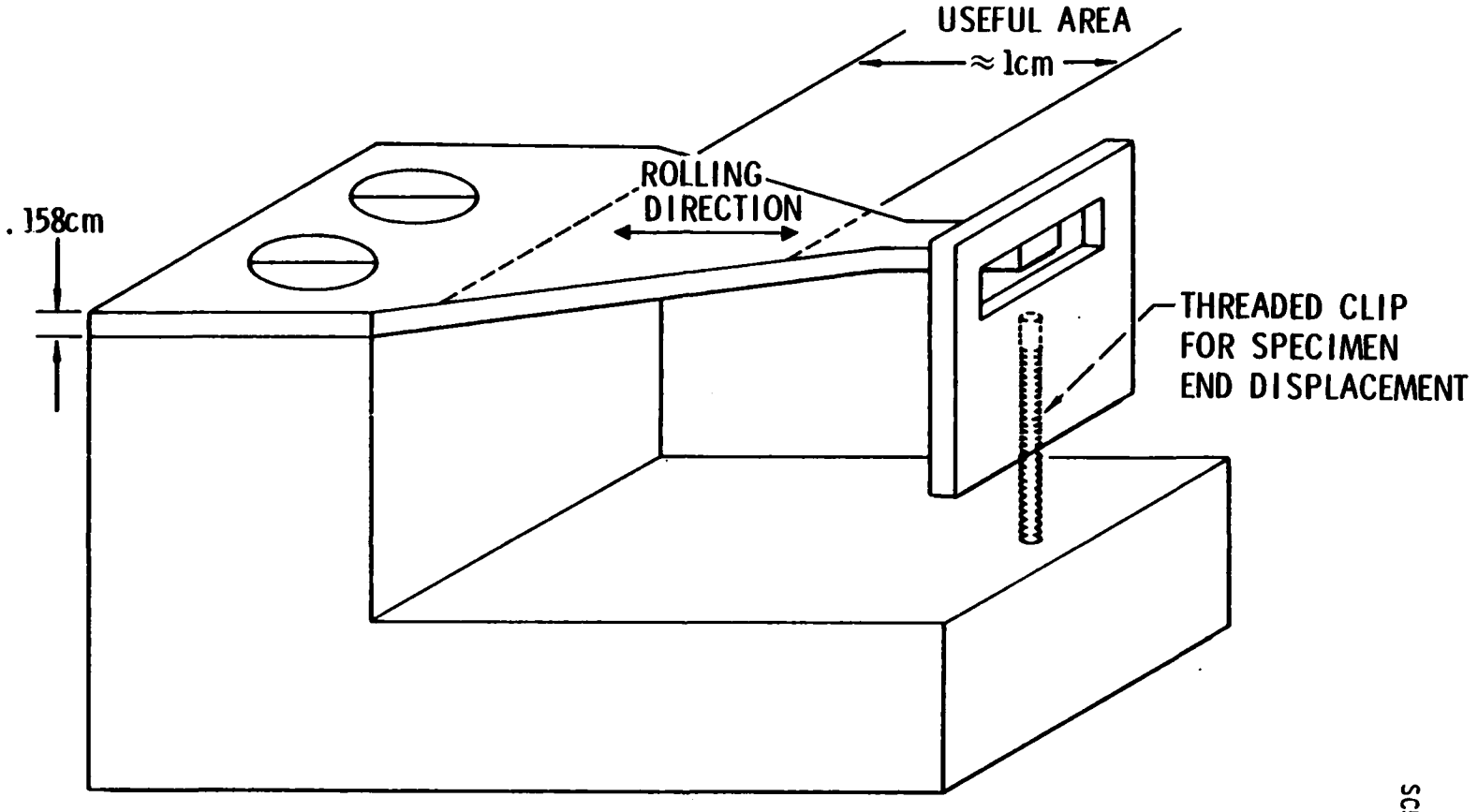

Fig. 2 Schematic illustration of fatigue specimen, shown in a jig used for loading the specimen in a scanning electron microscope.

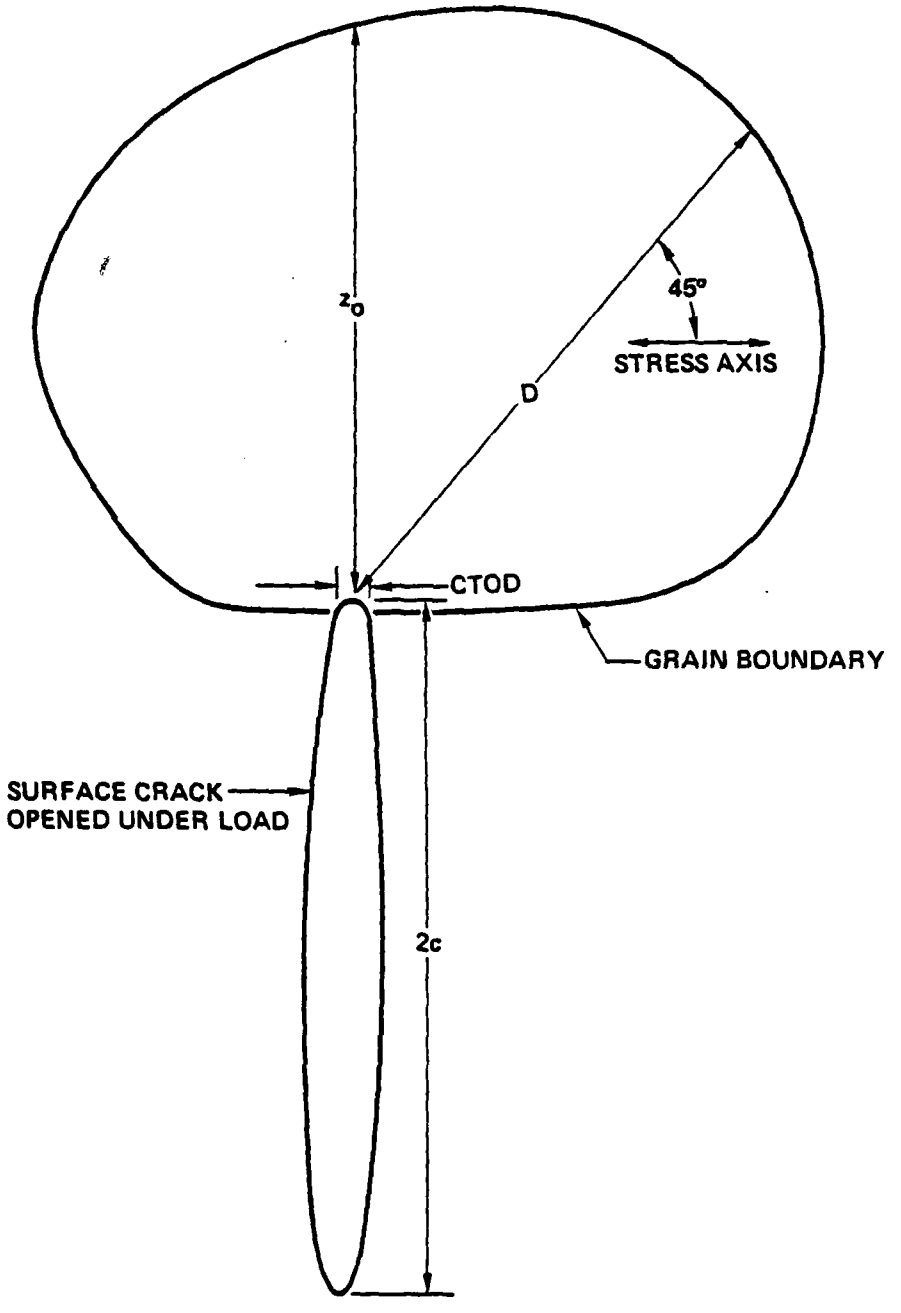

Fig. 3 Dimensional parameters used in determination of microplastic deformation. CTOD is found by extrapolation of displacements made near the tip to the tip as explained elsewhere.[3]

crystallographic cracks is entirely in the plane of the crack. A CTOD measurement on such cracks detects only the elastic opening normal to the crack path with the result that $CTOD/\delta(\sigma_{max}) \approx 0.1$, independent of z_o. Cracks which obviously were crystallographic were excluded from the data set in the 2219 and 7075 alloys. An extensive survey of surface cracks in Al 2024-T3 did not locate any non-crystallographic cracks. A possible alternative for crystallographic cracks is to measure displacements in the plane of the crack. Such an analysis is in progress.

As an interim step in development of a model of the dynamics of microplastic deformation at a surface crack tip, we assessed approaches to predict the equilibrium $CTOD_p$ and closure stress values encountered when plastic zone size is constrained by the grain boundaries. In Fig. 4 closure stress values predicted as a function of distance of crack tip to grain boundary, using two different models, are compared to experimental data. One prediction is obtained using a finite element analysis of the deformation at a crack tip with the plastic zone size constrained by a boundary. The second approach involves use of a superdislocation model of the deformation process. Details on both models are provided in Appendix B. A crack closure stress monotonically increasing with increased distance of the crack tip to the grain boundary is both observed and predicted. It appears that there is a tendency for some of the closure stress values to occur at systematically smaller values than expected with either model. We believe this is a result of the dynamics of plastic zone maturation as discussed next.

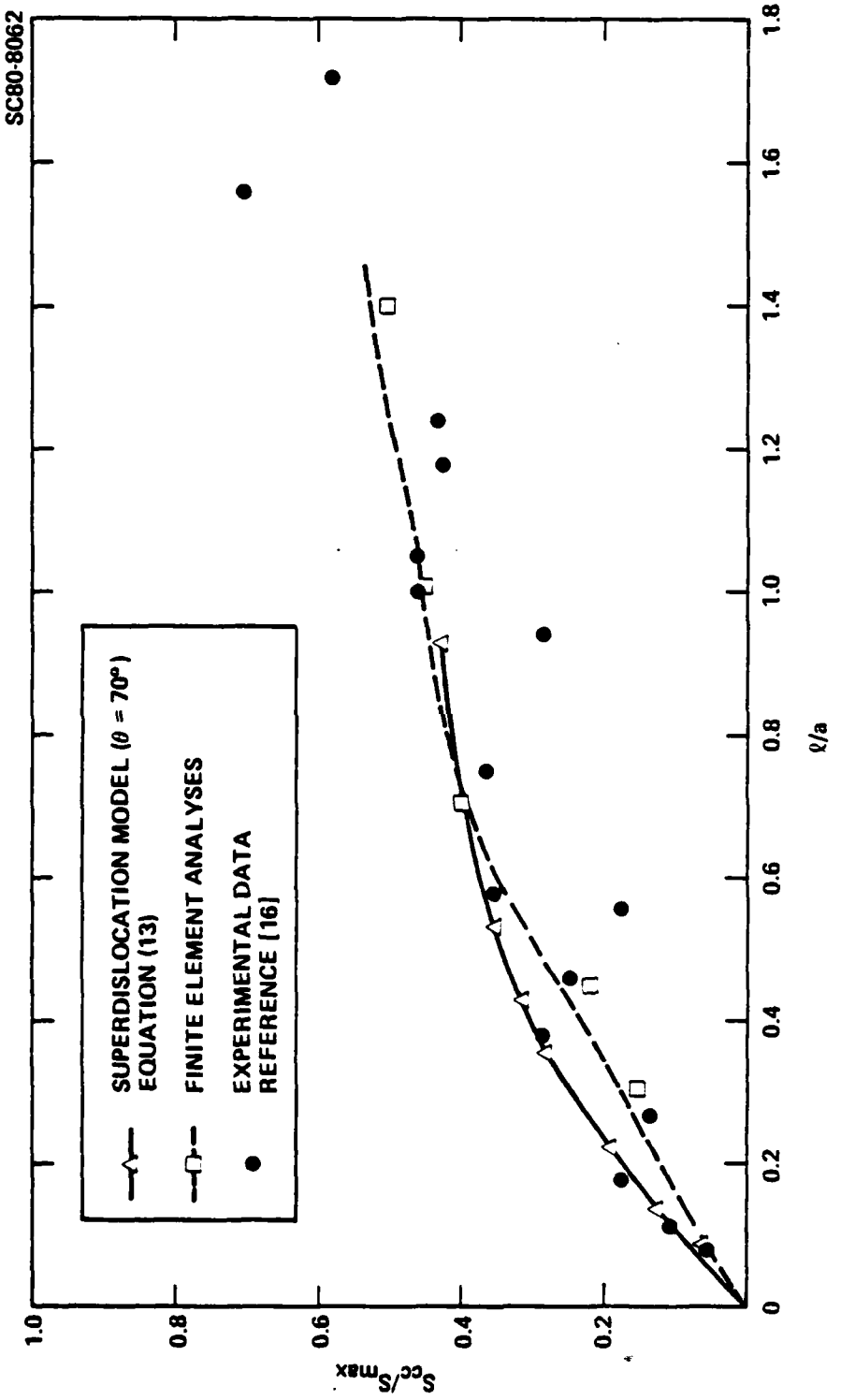

Fig. 4 Ratio of closure stress to maximum tensile stress increases with increased distance (ℓ) of crack tip to the next grain boundary. Here (a) is crack depth in a two dimensional crack model.

4.3 Dynamics of Plastic Zone Maturation

Once slip from a surface crack tip begins into a new grain, crack growth stops.[4,6] The duration of the incubation period is longer the smaller the cyclic stress amplitude. Using Al 2219-T851, a series of experiments were done to assess the dynamics of the incubation process by measuring CTOD vs fatigue cycles N for a large number of crack tips. Specimens were prefatigued at $\sigma_{max} = 0.9\ \sigma_{yield}$ to generate a distribution of short cracks. The cyclic stress amplitude was then lowered and the crack growth monitored at increments during fatigue. In particular we were hoping to locate cracks which initially continued to grow, but soon encountered grain boundaries at the lower stress amplitude and stopped. After an experiment was complete the surface was chemically etched to reveal the location and size of grains in the path of each crack tracked.

In Fig. 5 we show three results typical of such experiments. The data are plotted using the same format as in Fig. 1, and show a progressive increase in CTOD during fatigue, which illustrates the dynamics of accumulation of plastic deformation as a crack tip transits a grain boundary. In case A, both crack tips are undergoing incubation, and the crack length (2c) is constant during fatigue. The progressive increase in CTOD during fatigue parallels an increasing density of dislocations in the next grain with each fatigue cycle. Case B differs from case A only in that the other surface crack tip was not at a boundary and was propagating so that 2c increased progressively during fatigue. In case C, the applied stress was less than the friction stress required for deformation to begin into the next grain and the CTOD remained elastic. [We find that in the latter case ultimate

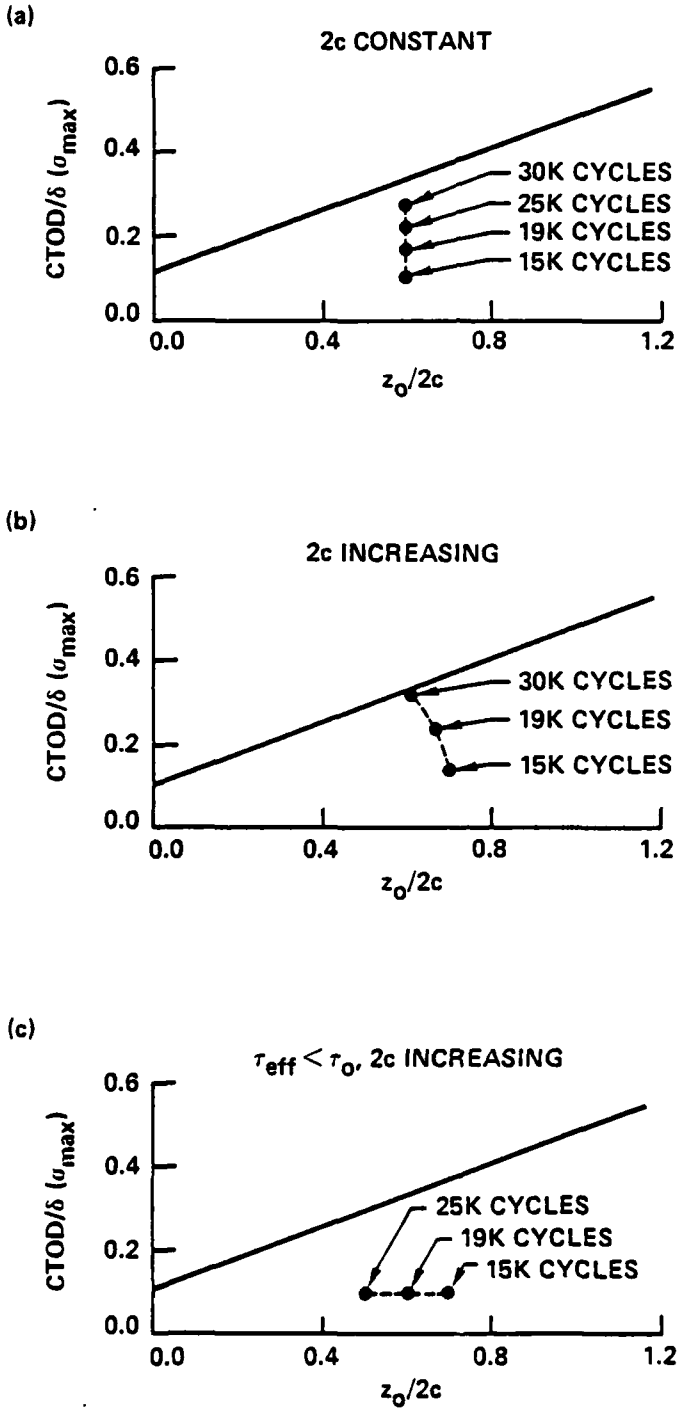

Fig. 5 Three examples of the progressive change in CTOD during incubation, for crack tips at grain boundaries.

propagation is typically intergranular and results from the fracture of grain boundaries ahead of but not directly connected to the main crack].

We propose expressions in Section 4.3.1 and 4.3.2 to predict:

1. The duration of the incubation period, ΔN_I, from which a coefficient θ describing the hardenability of the surface is determined.

2. The increase in the plastic component ($CTOD_p$) of CTOD during fatigue.

4.3.1 The Duration of the Incubation Period (ΔN_I) Before Commencement of Propagation

$$\int_{N_S}^{\Delta N_I + N_S} \xi D\sqrt{2c(N)}\,(\tau_{eff} - \tau_o)^2 e^{-2\theta N} dN = \beta. \qquad (2)$$

Eq. (2) is obtained from an analysis of the incubation process by Chang et al,[7] with several empirical modifications. ξ and β are material parameters. These are related to alloy ductility, as discussed later. D is the slip distance into the new grain and 2c(N) is the crack length after N fatigue cycles (Fig. 3). N_S is the number of fatigue cycles at which incubation began. We define an effective surface shear stress $(\tau_{eff} - \tau_o)e^{-\theta N}$ to replace the local stress S in the Chang derivation. Due to cyclic hardening of the surface the friction stress (τ_f) at the surface is assumed to increase at a rate proportional to the microplastic deformation at the surface. Thus

$$\frac{d\tau_i}{dN} = \theta(\tau_{eff} - \tau_i) \quad . \tag{3}$$

$$S = (\tau_{eff} - \tau_i) = (\tau_{eff} - \tau_o)e^{-\theta N} \quad . \tag{4}$$

θ is a coefficient of hardenability. τ_o is the friction stress in unfatigued material. τ_{eff} is an effective shear stress which is determined by the crystallographic orientation of the grain at the crack tip. τ_{eff} is constructed for a given grain orientation by calculating, from the applied stress, the shear stress in each of the (111) slip planes in the fcc aluminum. The largest component of these, lying both in a (111) plane and in the surface, is defined to be τ_{eff}.[8] (See Figs. 6 and 7).

In the special case that the crack length is constant during incubation and, if θ is small, Eq. (2) can be rewritten as

$$\ln[\Delta N_I D\sqrt{2c}] + \ln[(\xi/\beta)(\tau_{eff} - \tau_o)^2] = 2\theta N_S \quad . \tag{5}$$

A series of experiments were done to test Eq. (5), from which we could determine θ for selected alloys. Specimens were prefatigued in dry air to produce a set of surface cracks with a maximum length of about 150 μm. Several micrometers of the surface were then removed by mechanical polishing, to return the surface to an unhardened state. The surface was then chemically etched to reveal the grain boundaries, and duration of incubation periods for crack growth across grain boundaries was determined during subsequent

SC79-5962A

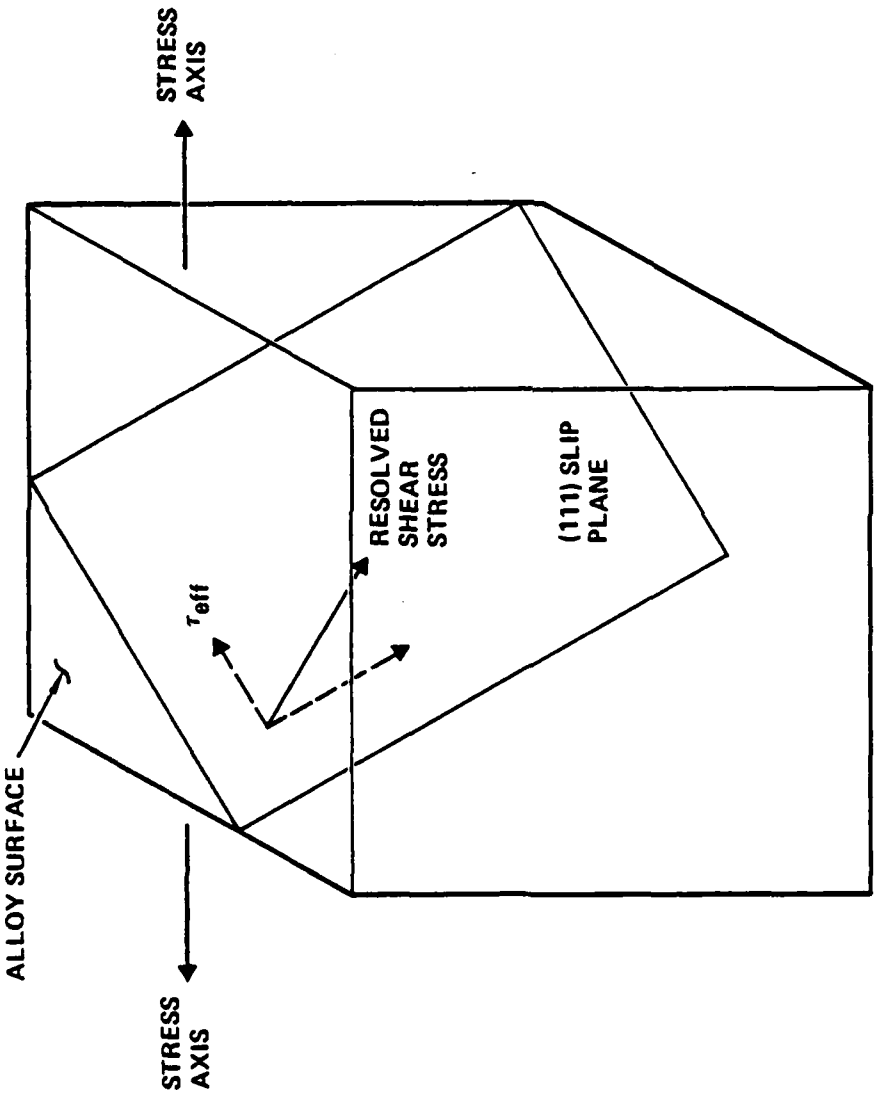

Fig. 6 Illustration of the projection scheme used in definition of τ_{eff}.

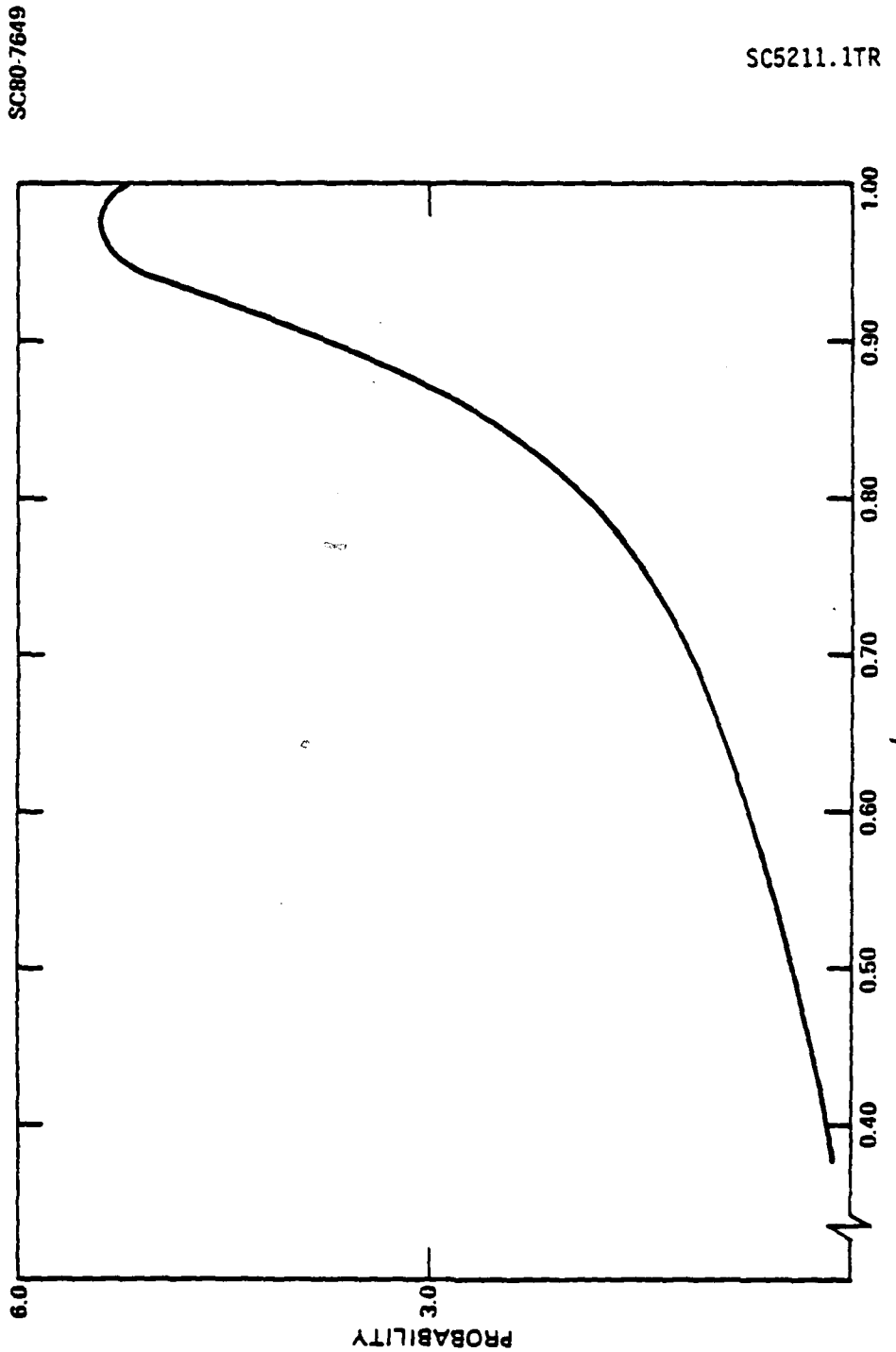

Fig. 7 Probability of occurrance of τ_{eff}, obtained by Monte Carlo selection of 30,000 random grain orientation. τ_{max} is the maximum applied surface shear stress.

fatigue. This was accomplished by making replicas of the surface at small intervals during fatigue, which were later examined to measure N_S, D, 2c and ΔN_I. Results for Al 2024-T3 for two humidities are shown in Fig. 8. θ is found from the slope of the incubation plot. Results for all materials studied to date are given in Appendix A. The effect of humidity is to increase the magnitude of θ. TEM of the dislocation structure near the surface of Al 2024-T3 show dislocation tangles in the alloy exposed to humid air, while zones of persistent slip are found on a specimen fatigued in dry air (Fig. 9).

4.3.2 $CTOD_p$ vs N

We obtained the theoretical dependence of $CTOD_p$ on number of fatigue cycles N using the model reported in Ref. 7, and by assuming that $CTOD_p$ is proportional to the number of dislocations in the slip band at the crack tip. Thus

$$CTOD_p = \frac{\varepsilon_y}{\beta} D^2\sqrt{2c}\,(N - N_s)(\tau_{eff} - \tau_o)^2 e^{-2\theta N} . \qquad (6)$$

We have assumed that the crack length is constant during incubation. An experimental test of Eq. (6) using Al 2219-T851 is shown in Fig. 10. The progressive increase in $CTOD_p$ with fatigue illustrates the physical reality of the incubation process. Numerous examples of the effect have been studied of which Fig. 10 is typical.

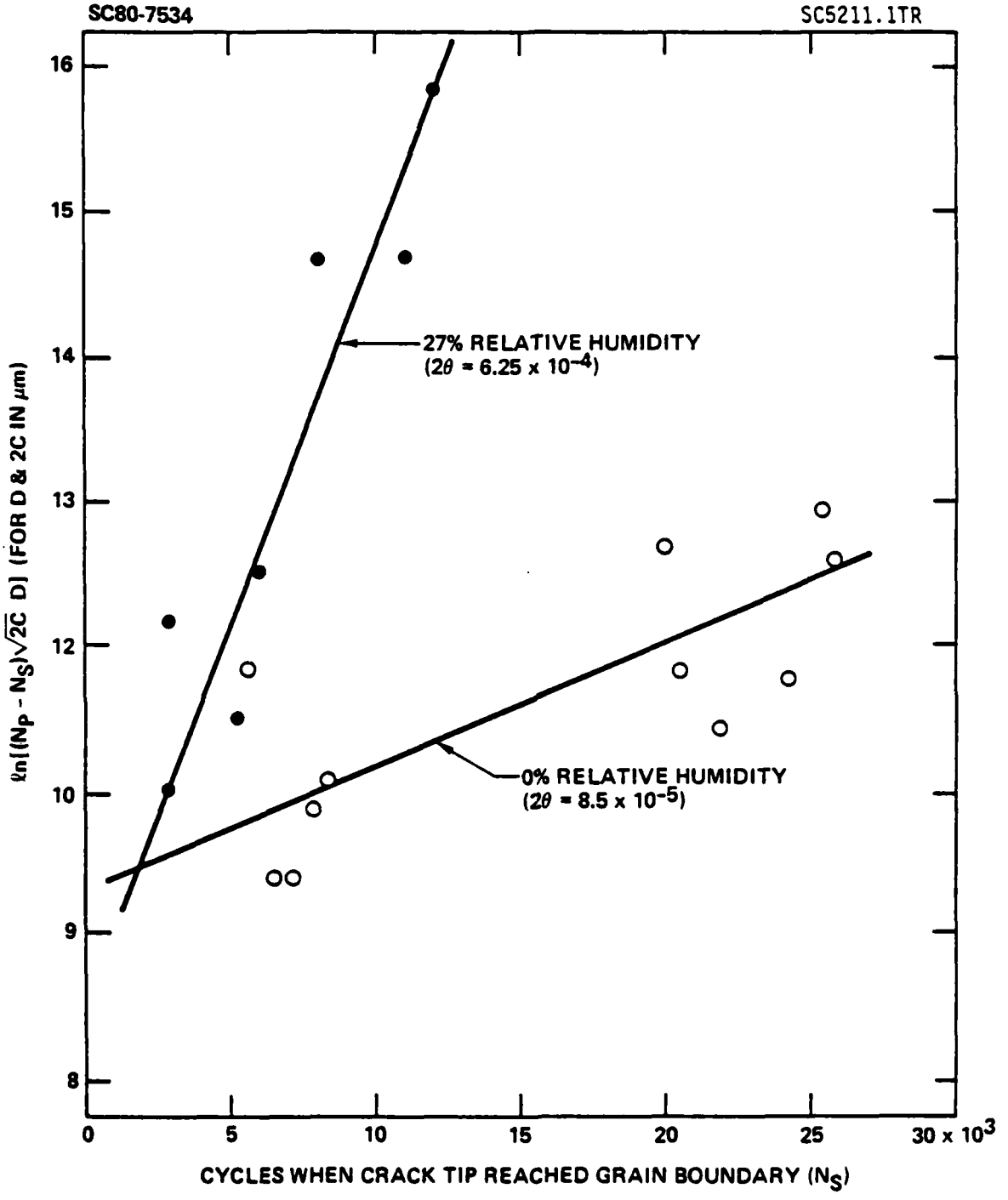

Fig. 8 Duration of incubation $\Delta N_I = N_p - N_s$ increases for cracks which reach grain boundaries later in fatigue (N_s).

SC80-9933

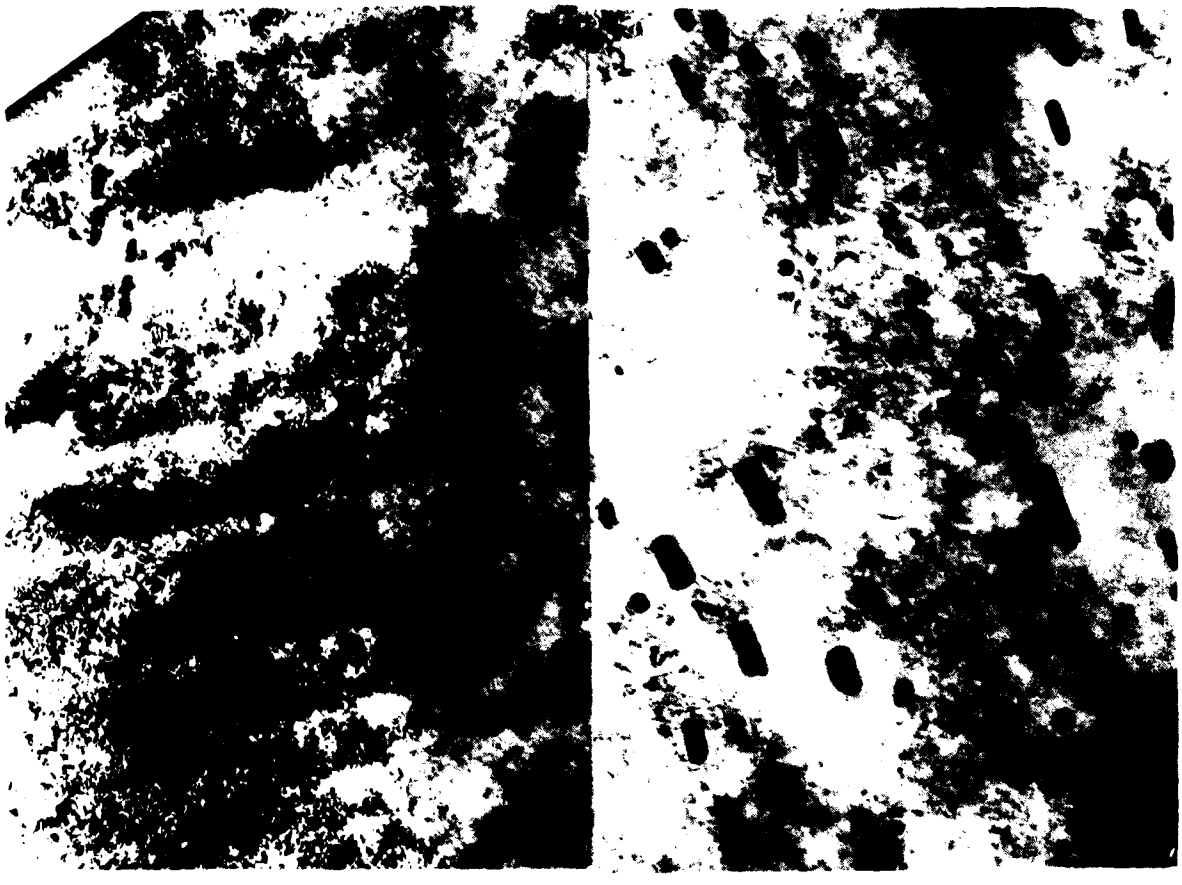

Fig. 9 Micrograph at left shows banded slip in dry air, at right dislocation tangles in humid air. Magnification X40,000.

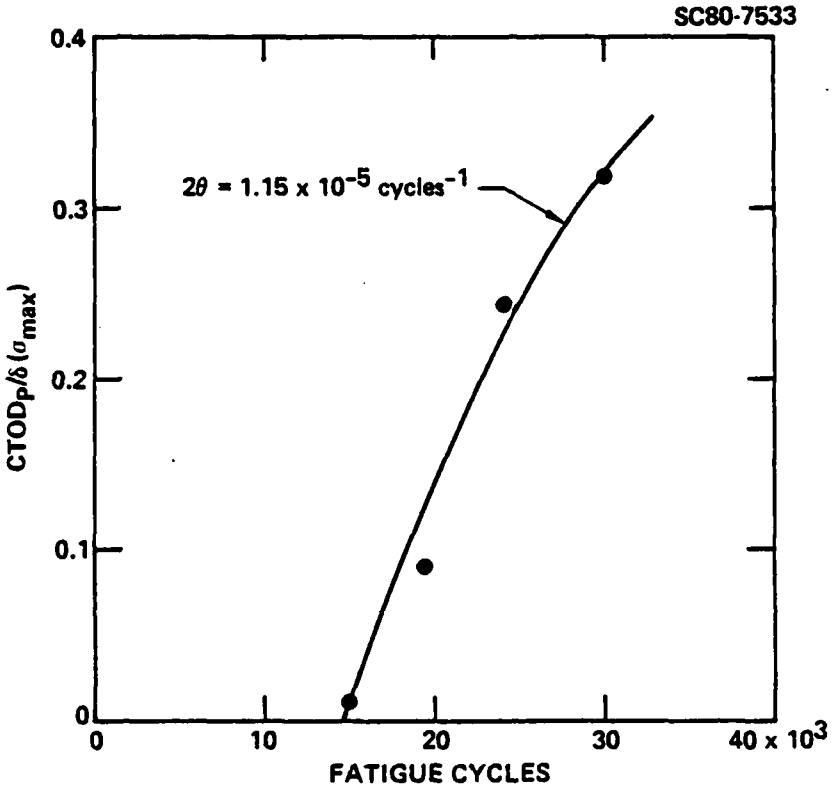

Fig. 10 Progressive increase in $CTOD_B$ for crack tip which reached a boundary at 15 × 10^3 fatigue cycles.

5.0 NEW INSIGHT INTO SURFACE DUCTILITY

The ductility of the surface of aluminum alloys changes progressively during fatigue. Surface hardening occurs both in dry and in humid air, but is much more rapid and greater in magnitude in humid air.[6] The effect of the hardening is seen both in the crack initiation and in the early growth behavior of the alloys. For instance, in Al 2219-T851 humidity decreases the numbers of intermetallic particles which fracture during fatigue. Furthermore, humidity decreases the rates at which residual surface stress, induced by machining in Al 2219-T851, relax during fatigue.[11] [Figures 11 and 12 which illustrate the effect of cyclic hardening of the surface on particle fracture and relaxation of residual stress were obtained in a Rockwell IR&D supported investigation.] Both these effects are attributed to the reduction in microplastic deformation per cycle which results from an environmentally assisted increase in friction stress of the near surface material.

During early crack propagation the effect of ductility on growth rate is complex. Slip which promotes propagation for fatigue amplitudes below the yield strength does not extend in substantial amounts beyond a grain boundary until a surface crack tip approaches the boundary. Propagation ceases at the boundary until a mature plastic zone is developed in the new grain. We refer to this process as incubation. Propagation rate after incubation is complete is controlled by the closure stress at the surface crack tip, which is a function of the grain size and of the ductility of the alloy at the surface. The effect of a decreased ductility during fatigue in humid air is to increase

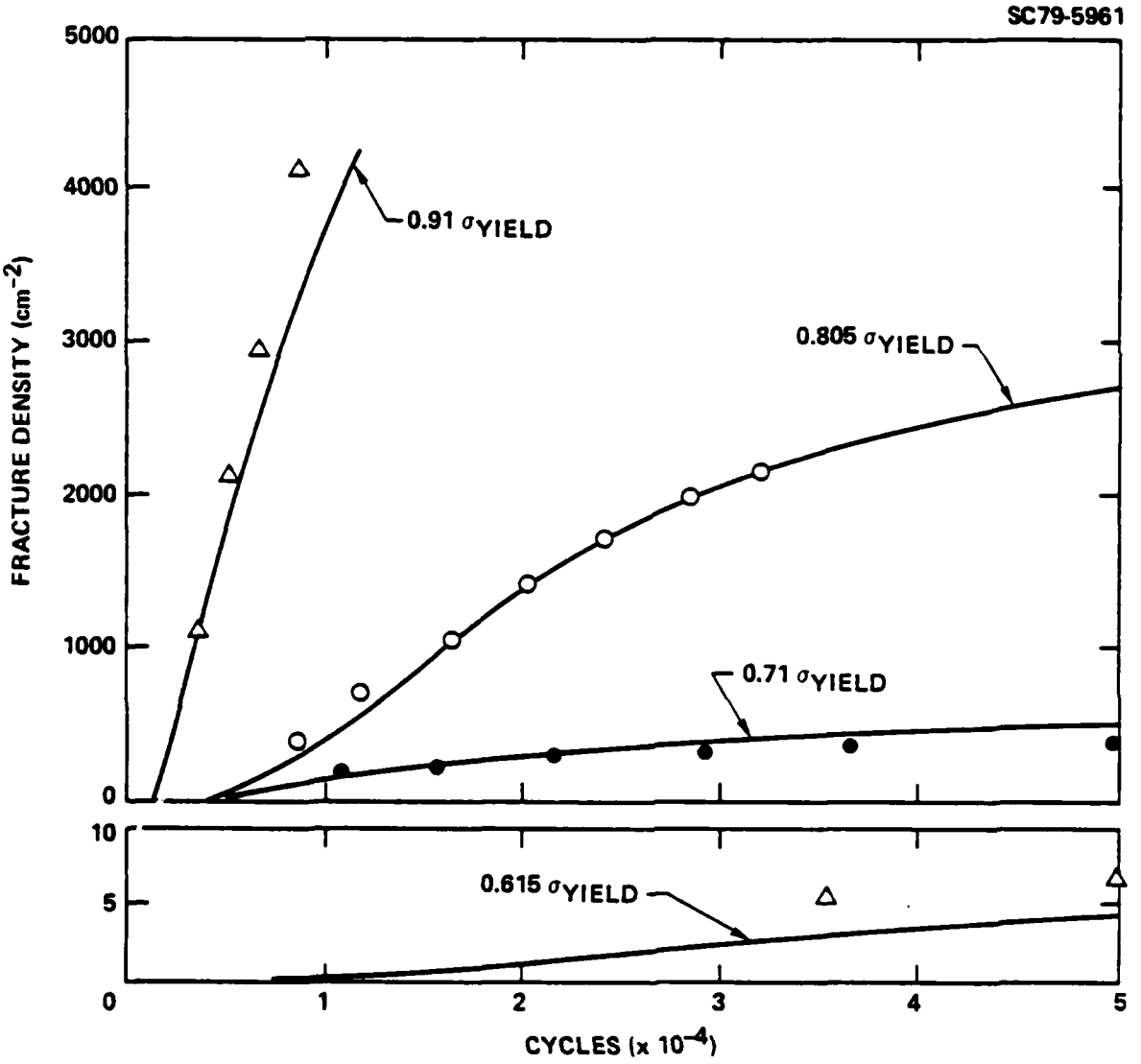

Fig. 11 Density of particles fractured on the surface of Al 2219-T851 during fully reversed fatigue for four maximum cyclic stress amplitudes. Symbols are experimental data obtained by SEM. Curves are computer predictions. Decrease rate of fracture later in lifetime is due to cyclic hardening of the surface and is more pronounced for fatigue in humid than in dry air.

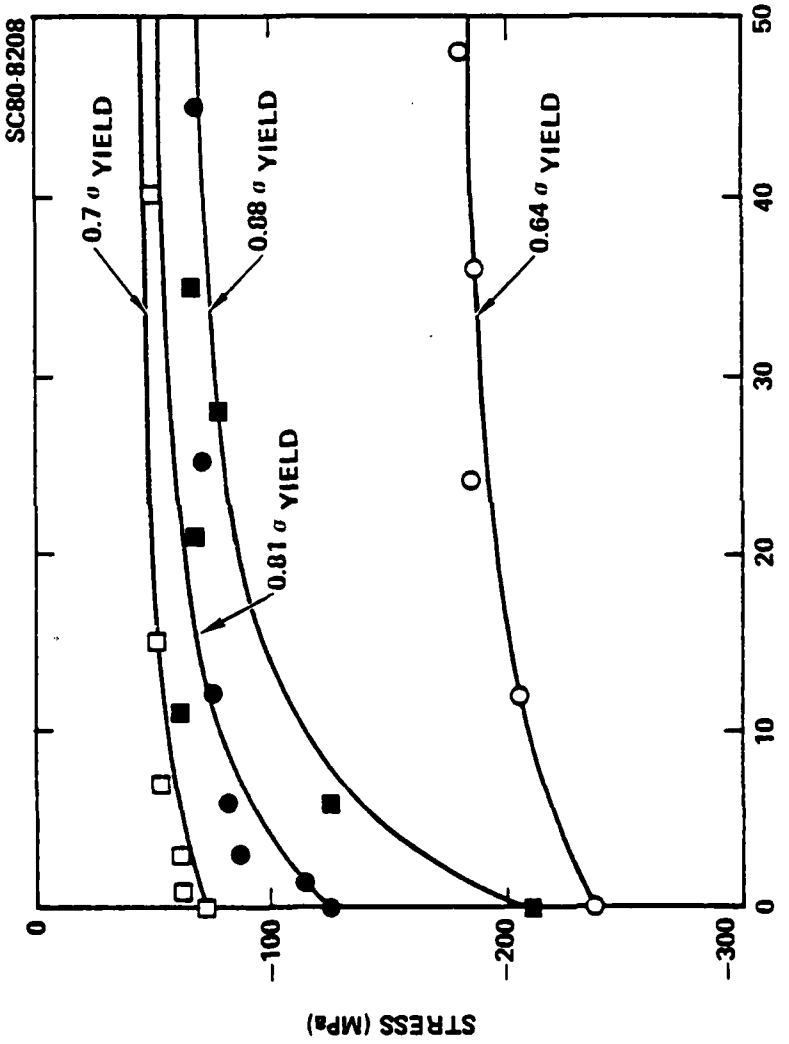

Fig. 12 Compressive residual stresses induced in Al 2219-T851 by machining decrease in magnitude during fatigue at a rate determined by the initial stress value and by the cyclic stress amplitude. Symbols show experimental values for four different residual stress/external stress amplitude states. Saturation of relaxation occurs when hardening of the surface raises the friction stress to the applied stress as seen in model predictions (curves). Relaxation is more rapid in dry air, for which there is less cyclic hardening of the surface.

the incubation period and to decrease the closure stress, leading to accelerated rates of propagation after incubation. The net effect of ductility on lifetime is therefore determined by the distribution in size of the grains at the alloy surface.

We also find that surface hardening has no appreciable effect on crack nucleation at grain boundaries. We conclude that slip leading to cracking of particles and slip which accompanies microcrack propagation is long range, extending across the grain matrix to the grain boundaries. Grain boundary cracking involves void nucleation, requiring only short range deformation.[12] Models based upon this view have been highly successful in predicting crack initiation and growth behavior in Al 2219-T851.[4,6,8] We believe that this situation pertains to high strength aluminum alloys in general.

The effect of humidity is to reduce the propensity for long range slip. TEM of near surface dislocation structure shows banded slip in an Al 2024-T3 alloy fatigued in dry air and dislocation tangles in humid air (Fig. 9). Surface hardening is treated theoretically by the introduction of a friction shear stress τ_o, altered during fatigue at a rate determined by, θ, a hardenability coefficient.

Our approach to measuring surface ductility has been to recognize that early crack growth behavior is affected both by geometrical factors (grain size, crack length, crack location) and by the ductility of the surface. We have formulated relationships through combinations of models and

empirical observations which allow us to relate measurables to the geometrical parameters and to the desired ductility parameters. By this means we find that five distinct material parameters are required to describe the behavior of an aluminum alloy surface, as affected by humidity. These are:

1. Parameter θ, which describes the increase in friction shear stress τ_0, during fatigue.

2. Parameter ξ, which specifies the rate of increase in dislocation density in a slip band at a crack tip with cyclic strain.

3. Parameters β and ε'_y, which are related to a critical strain energy density for propagation and an ultimate material strength respectively.

All five parameters are independent of N and of alloy grain size, and two are known to be functions of humidity. (By defination τ_0 is independent of humidity, since any humidity dependence is carried in θ). θ is larger and ε'_y is smaller in moist air than in dry air. The effect of humidity on β and ξ remains to be established, as do the effects of alloy composition and heat treatment on these parameters. Initial results suggest, however, that θ is much more sensitive to humidity in underaged alloys.

The incubation model is based upon a "small deformation" theory. The increase in the friction stress during fatigue has been incorporated

empirically into the model to explain the progressive hardening of the surface manifested in both crack initiation in early growth behavior observed in 2000, 6000 and 7000 series alloys. Our superdislocation model of CTOD relies upon a large deformation analysis to predict equilibrium values of CTOD and of crack tip closure stress. These two methods both predict that a critical strain energy density at the crack tip is required for propagation. We denote this effect by the parameter β for the incubation model and the parameter ε_y' for the CTOD model. The interrelationship between β and ε_y' remains to be determined. The cycle dependence of CTOD during incubation is also potentially rich in information about surface ductility, but our new model of this process must be tested before it can be generally applied. The status of what can presently be measured regarding ductility is summarized in Table 1.

Table 1

Summary of Ductility Measurements

Process/ Parameter	Measurement		
	Incubation Period	CTOD vs N Dependence	CTOD Equilibrium Value
Increase in $\tau_o/(\theta)$	Measured using Eq. (5)	Measured using Eq. (6)	Not expected to directly affect equilibrium CTOD
Rate of increase of dislocation density with cyclic strain/ (ξ)	The ratio ξ/β measured using Eq. (5)	$\frac{\varepsilon'_y}{\beta}$ measured using Eq. (6)	Not expected to directly affect equilibrium CTOD
Critical strain energy density for propagation/ (β, ε_y)	The ratio ξ/β measured using Eq. (5)	$\frac{\varepsilon'_y}{\beta}$ measured using Eq. (6)	ε'_y measured using Eq. (1)

The three material parameters ξ, (β, ε'_y) and θ each describe a different facet of ductility, but it is likely that they are partially interrelated. This prospect will require a further improvement in understanding of the nature of near surface deformation in aluminum alloys. Hopefully, in the second year of research, a unified theory of surface ductility will be forthcoming. Intuitively, each parameter represents a different aspect of ductility such as might be encountered in a macroscopic evaluation of alloy ductility. (β, ε'_y) is similar to a large deformation, reduction in area parameter. Materials with large (β, ε'_y) are more ductile and will sustain more strain at a microcrack tip before separation. Hardening or softening of the bulk material during fatigue is common and can arise from dislocation

mechanisms. Parameter θ describes the rate of surface hardening, which is highly sensitive to presence of humidity for aluminum alloys. The depth of material at the surface affected by environment is very shallow, on the order of several microns, as suggested by the amount of material which must be removed to return the surface to an unhardened state. Parameters ξ and τ_0 are distantly related to the microplastic stress-strain response of a material, which can be determined for bulk material. Because the slip important to early crack growth is confined to a thin layer near the surface, however, (β, ε_y'), θ and ξ are all sensitive to humidity and to the partial relaxation of bulk constraints on deformation at the surface.

6.0 DISCUSSION AND SUMMARY

It has been many years since Frost[13] first concluded that the plain fatigue limit was a function of grain size and that crack propagation across grain boundaries required lower cyclic stress amplitudes the larger the grain hence the larger the initial crack size. Forrest and Tate[14] determined that an empirical expression proposed by Frost, which related crack length to the cyclic stress amplitude required for propagation, required only a slight modification to describe the effect of grain size on the fatigue limit of a 70/30 brass. Later Hoeppner[15] showed that for stress amplitudes above the fatigue limit a smaller grain size suppressed propagation across grain boundaries for more fatigue cycles than a large grain size. Thus Hoeppner observed the process we refer to as incubation. Taira, Tanaka and Nakai[16] have proposed a model of the fatigue limit based upon a derivation which shows that, below a critical stress amplitude, slip from a crack tip does not proceed across a boundary into the next grain. By assuming propagation across the boundary requires slip into the new grain, they derive a dependence of the fatigue limit upon grain size which appears adequate to explain experimental observations of the effect of grain size on fatigue limit in a low carbon steel.[17] The model of the incubation process proposed by Chang et al.[7] distinguishes the effects of crack length from that of grain size at the crack tip. It differs from the model in Ref 16 in that it addresses crack propagation as well as the fatigue limit. It presumes that slip into the next grain is <u>necessary</u> but <u>not sufficient</u> for propagation, and that in addition

sufficient microplastic deformation must accrue for propagation. The Chang model predicts a fatigue limit (τ_f) for intergranular crack propagation of the form

$$\tau_f = \text{constant } \sqrt{\theta/D} + \tau_o \, . \qquad (7)$$

There are, thus, three separate equations [Eq. (2), (5) and (7)] related to various aspects of the incubation process, which require evaluation. Of these Eq. (2), and its approximate representation Eq. (5), has been subjected to the most scrutiny. The effect of grain size, crack length and hardenability on the duration of the incubation period appears to be correct. The dependence upon stress amplitude is known to be approximately correct but has not been tested rigorously. The effect of crystallographic orientation on the incubation period has been verified using a statistical analysis but not by direct measurement of the crystallographic orientation of a grain at a crack tip.[8] We know the duration of incubation is correctly described by Eq. (2) if propagation into the new grain is transgranular and either crystallographic on non-crystallographic. We do not know, however, if (β/ξ) is the same for both crystallographic and noncrystallographic cracks in the same alloy. Furthermore we have not looked for a possible effect of crack depth (as compared to crack length) on the duration of incubation.

In regard to prediction of $CTOD_p$ [Eq. (6)] only the dependences upon θ and N have been tested and these appear correct. It can be argued that, since Eqs. (2) and (6) come from the same root equation, their dependencies

upon D and 2c should be equally valid. However, we would not be surprised if this were not the case, considering the many assumptions and approximations in the theory. Evaluation of Eq. (6) is extremely tedious owing to the difficulty of measuring $CTOD_p$ vs N. In the alloys studied to date, Eq. (6) is invalid for crack lengths longer than ≈ 300 μm, for which length deformation at the crack tip is determined by continuum constraints.

In regard to Eq. (7), we have serious doubts of its applicability to aluminum alloys. The 2000 series aluminums on which we have consentrated the majority of our research do not have an endurance limit. At low stress amplitudes crack growth at the surface is intergranular and Eq. (7) can not be expected to apply. The growth process in this case involves fracture of grain boundaries ahead of but not directly connected to the crack tip, followed by linking of the secondary cracks with the main crack. We have measured the CTOD of the main crack and find that intergranular cracking can occur even if the cyclic hardening has proceeded to the point that the CTOD remains elastic. It, thus, appears that the fracture of grain boundaries ahead of the crack tip can result from strain amplification due to the elastic strain associated with the main crack. Perhaps Eq. (7) might apply to alloys which have a true endurance limit such as certain steels.

In summary, the models from which ductility parameters have been defined and calculated are not completely tested. Indeed, given the multiplicity of microstructural parameters involved it is not likely that at a complete evaluation of the equations will be forth coming under this contract. Furthermore, the mechanism of hardening of the surface is not

presently known, although we suspect that it may result from the effect of the oxide layer on the dislocation structure near the surface. Grosskreutz[18] has reached such a conclusion for Al 1100 alloy. However, the ductility parameters have demonstrated utility in predicting several aspects of fatigue behavior. The parameters must be viewed as empirical quantities until model verification is complete and mechanisms are further defined. Until then they serve as useful evaluators of the sensitivity of materials to fatigue failure, and guide in determination of the effect of alloy chemistry and heat treatment on fatigue behavior in humid air.

7.0 REFERENCES

1. W. L. Morris, O. Buck and H. L. Marcus: Met. Trans. A, p. 1161, 1976.

2. W. L. Morris and O. Buck: Met. Trans. A, 8, p. 597, 1977.

3. W. L. Morris: Met. Tran. A, 11, p. 1117, 1980.

4. W. L. Morris, M. R. James and O. Buck: "Growth Rate Models for Short Surface Cracks in Al 2219-T851," scheduled for publication in Met. Trans.A.

5. W. L. Morris and O. Buck: "Environmental Effects on Fatigue Crack Initiation," Final Report on Contract No. N00014-76-C-0452, for the Office of Naval Research.

6. M. R. James and W. L. Morris: "Quantitative Modeling of Fatigue Crack Initiation," submitted to Mat. Sci. and Eng.

7. R. Chang, W. L. Morris and O. Buck: Scripta Met. 13, p. 191, 1979.

8. W. L. Morris and M. R. James: Met. Trans. A, 11, p. 850, 1980.

9. J. R. Rice: "Mechanics of Crack Tip Deformation and Extension by Fatigue," Fatigue Crack Propagation, ASTM STP 415, Am. Soc. Test and Mat. p. 247, 1967.

10. A. E. Green and I. N. Sneddon: Proc. Cambridge Phil Soc., 46, p. 159, 1950.

11. M. R. James and W. L. Morris: "The Relaxation of Machining Stresses in Aluminum Alloys During Fatigue," in Residual Stress for Designers and Metallurgists, ASM Conf., Chicago, Ill., April 9-10, 1980 (in press).

12. R. Chang: Scripta Met. 13, pp. 1079, 1979.

13. N. E. Frost: Proc. Inst. Mech. Eng, 173, p. 811, 1959.

14. P. G. Forrest and A. E. L. Tate: Journal Inst. Met, 93, p. 438, 1964.

15. D. W. Hoeppner: Fatigue Crack Propagation, ASTM 415, Am. Soc. Testing Materials, p. 486, 1967.

16. S. Taira, K. Tanaka and Y. Nakai: Mech. Res. Comm., 5, p. 375, 1978.

17. Y. Nakai and K. Tanaka: In Proc. 23rd Japan Congress on Matrials Research, 1980 in Press.

18. J. C. Grosskreutz: Surface Sci. 8, p. 173, 1967.

19. R. Chang: "On Crack Closure Phenomena in Fatigue," submitted Int. J. Fract.

APPENDIX A

EXPERIMENTAL DUCTILITY PARAMETER VALUES

Alloy	Humidity, %	ε_y'	θ, cycles^{-1}	β/ξ, MN/$\sqrt{m}$	τ_0, MN/m^2
Al 2215-T851	0	0.36	1×10^{-5}*	-	182
Al 2215-T851	60	0.25	3×10^{-5}	1.9×10^{-2}	182
Al 2024-T3	0	-	4.2×10^{-5}	0.9×10^{-2}	-
Al 2024-T3	27	-	3.1×10^{-4}	0.9×10^{-2}	-
Al 2024-T6†	50	-	$<1 \times 10^{-5}$	2×10^{-1}	-
Al 7075-T6	50	0.40	3.5×10^{-5}	1.7×10^{-1}	-

*A second heat of Al 2219-T851 has been found for which $\theta << 1 \times 10^{-5}$ and is independent of humidity. The relationship of θ to alloy composition is now being assessed.

†Commercial T3 material, aged to peak hardness.

APPENDIX B (REF. 19)

ON CRACK CLOSURE PHENOMENON IN FATIGUE

Roger Chang
Rockwell International Science Center
Thousand Oaks, California 91360

ABSTRACT

The crack closure phenomenon in fatigue under plane strain is studied by means of an inclined strip yield superdislocation model and finite element stress analysis, with particular emphasis on the effect of plastic zone constrain on crack closure. Both analyses show that the crack closure stress (normalized with respect to the maximum applied stress) increases almost linearly with ℓ/a at low ℓ/a values and rises more slowly with increasing ℓ/a ratio at larger ℓ/a values (ℓ being slip band length, a the half crack width).

I. INTRODUCTION

Since Elber's [1,2] discovery of the crack closure and the introduction of the effective stress-intensity range, $\Delta K_{eff} = K_{max} - K_{op}$, where K_{max} is the maximum stress-intensity factor and K_{op} is the stress-intensity factor at which the crack opens, there have been many studies, both experimental and theoretical, on crack closure and its effect on fatigue crack growth. While some investigators [3] provided experimental evidence that crack closure is a surface effect, others [4-6] concluded that closure is a general phenomenon. There also

have been studies [7,8] which indicate that crack closure can be quite pronounced in the threshold region where the shear fracture mode is prevalent, but the arguments presented are not conclusive. Comprehensive theoretical analyses of closure in fatigue crack growth based on the Dugdale model in plane stress case have been reported recently [9-11]. There is a need to perform similar theoretical analyses under plane strain conditions. This is one of the principal purposes of the present study. Numerical analyses of crack closure employing both the inclined strip yield superdislocation model [12-14] and a finite element method were used in this investigation. Another objective of this study concerns the crack closure behavior in polycrystalline materials where an advancing microcrack runs toward a grain boundary or similar obstacle which restricts the slip band length and/or plastic zone size to the dimension between the advancing crack tip and the obstacle. Literature is rich in experimental information concerning the effect of grain size on fatigue crack closure [15,16]. A theoretical understanding of the experimental observation on grain size effects is important to the kinetics of fatigue crack nucleation and growth in real materials.

II. INCLINED STRIP YIELD SUPERDISLOCATION ANALYSES

The inhomogeneous plastic strain produced at a crack tip can be advantageously represented on a microscale by dislocation arrangements, where the maximum shear stresses are symmetrically located on planes inclined at some angle to the crack. Bilby and Swinden [17] first reported the results of

numerical calculations for dislocations inclined at 45° to the crack plane. Vitek [18] and Riedel [19] have recently obtained more comprehensive results for slip planes inclined at various angles. The basic equations for the representation of crack tip plasticity based on an inclined strip yield superdislocation model have been derived by Atkinson and Kanninen [12,13] and used by Evans [14]. The complex variable approach of Muskhelishvili [20] was adopted by these investigators. For the crack and slip superdislocation configuration shown in Fig. 1, the crack of width 2a lies along the X-axis with the tips of the crack situated at the positions (a,o) and (-a,o), respectively. The superdislocation n, where n = 1 to m, situated at positions $Z_n = a + \ell n \exp(i\theta)$ with Burgers vectors B_n, experiences a shear stress τ_n given by each of the m discrete superdislocations,

$$\tau_n = SH_n + \frac{\mu}{4\pi(1-\gamma)} \sum_{j=1}^{m} B_j (G_{nj} + K_{nj}), \qquad n = 1,2 \ldots m \tag{1}$$

S is the applied tensile stress normal to the crack plane, μ is the shear modulus, γ is the Poisson's ratio, B_j is the Burger's vector of the j^{th} superdislocation and the remaining terms are defined below (see Eqs. (7), (8) and (9)). It is assumed that the material has an intrinsic resistance to superdislocation motion along the slip plane, denoted by τ_i (the friction stress). The equations of force equilibrium that form the basis of the mathematical model are formed by replacing τ_n of Eq. (1) by τ_i for each of the m superdislocations.

In general, the interaction between the crack, applied stress, and the superdislocations produces a stress field behaving like $K_I/\sqrt{2\pi r}$ near the crack

tip, where r is the distance from the crack tip and K_I is the mode I stress-intensity factor given by,

$$K_I = S\sqrt{\pi a} - K_i \tag{2}$$

K_i is the component of the stress-intensity factor that results from the effect of the stress fields of the superdislocations acting on the crack.

$$K_i = \frac{\mu}{4\sqrt{\pi a}(1 - \gamma)} \sum_{j=1}^{m} B_j F_j \tag{3}$$

where F_j is defined below (see Eq. (10)) and the other terms are as defined previously. The component of stress containing the square-root singularity can be suppressed by setting

$$S = \frac{\mu}{4\pi a(1 - \gamma)} \sum_{j=1}^{m} B_j F_j \tag{4}$$

In our representation of the crack tip plasticity, only a single superdislocation rather than m superdislocations was used. This representation is justified for the following reasons. First, extensive calculations employing m superdislocations, where m is a variable integer used in the manner of Atkinson and Kanninen [12,13] and Evans [14], failed to yield any more understanding than that according to a single superdislocation representation. Furthermore, numerical solution of the force equations becomes considerably more simplified with the single superdislocation representation. In the single

superdislocation representation, m = 1, Eqs. (1) and (4) are reduced to

$$\tau_i = SH + \frac{\mu}{4\pi(1-\gamma)} B\,(G + K) \tag{5}$$

$$S = \frac{\mu}{4\pi a(1-\gamma)} BF \tag{6}$$

The parameters H, G, K and F in Eqs. (5) and (6) for a single superdislocation with Burger's vector B situated at $Z = a + \ell \exp(i\theta)$ are given by [12],

$$H = \sin\theta\left\{\cos\theta + a^2\ell\,\mathrm{Re}\left[\frac{e^{2i\theta}}{(Z^2 - a^2)^{3/2}}\right]\right\} \tag{7}$$

$$G = 2\ell\sin^2\theta\,\mathrm{Re}\left\{\frac{e^{2i\theta}}{(Z^2-a^2)^{1/2}}\left[\frac{Z(\bar{Z}^2-a^2)^{1/2}}{(Z^2-a^2)(Z-\bar{Z})} - \frac{2Z^2+a^2}{2(Z^2-a^2)^{3/2}}\right.\right.$$

$$\left. + \frac{(\bar{Z}^2-a^2)^{1/2} - (Z^2-a^2)^{1/2}}{(Z-\bar{Z})^2}\right] + \frac{\ell\,e^{2i\theta}}{(Z^2-a^2)^{1/2}}\left[-\frac{a^2 Z\,e^{i\theta}}{(Z^2-a^2)^{5/2}}\right.$$

$$\left.\left. + \frac{e^{-i\theta}}{(Z-\bar{Z})^2(\bar{Z}^2-a^2)^{1/2}}\left(\frac{a^2(Z-\bar{Z})}{Z^2-a^2} + 2\,\frac{(Z^2-a^2)^{1/2}(\bar{Z}^2-a^2)^{1/2} + a^2 - Z\bar{Z}}{Z-\bar{Z}}\right)\right]\right\} \tag{8}$$

$$K = -\frac{\cos 2\theta}{\ell} \tag{9}$$

$$F = 4 \sin\theta \left\{ \mathrm{Re}\left[\frac{(Z^2 - a^2)^{1/2}}{Z - a}\right] + a\ell\, \mathrm{Re}\left[\frac{e^{i\theta}}{(Z - a)(Z^2 - a^2)^{1/2}}\right] \right\} \tag{10}$$

where Re is the real part of and $\bar{Z}$ is the complex conjugate of Z.

For small scale yielding, $\ell \ll a$, the above equations are further simplified. Atkinson and Kanninen [12] and Evans [14] treated their cases in small scale yielding approximation. However, for slip band length ℓ of the order of half crack width a, small scale yielding approximation is no longer applicable and the full expressions given by Eqs (7) to (10) must be used.

When the applied stress S is reduced by ΔS to $(S - \Delta S)$, there is a tendency for the dislocations to move back toward the crack, but the movement will be resisted by the friction stress. Only those dislocations lying between $\ell = 0$ and $\ell = \ell_r$ (where ℓ_r is the reversed plastic zone dimension) will actually move. When a new equilibrium is established, the dislocations in the reversed plastic zone will experience a friction stress equal to $-\tau_f$. Within the region $0 < \ell < \ell_r$, the net strength of the dislocations becomes $(B - B_r)$, and Eq. (5) becomes

$$-\tau_f = (S - \Delta S)H + \frac{\mu}{4\pi(1 - \gamma)} (B - B_r)(G + K) \tag{11}$$

Taking the difference between Eq. (5) and Eq. (11), one obtains

$$2\tau_i = \Delta SH + \frac{\mu}{4\pi(1-\gamma)} B_r (G + K) \qquad (12)$$

where B_r can be viewed as the contribution to dislocation distribution from the reversed shear as a result of the lowering of applied stress from S to (S - ΔS). When $\Delta S = S$, or $(S - \Delta S) = 0$, B_r from Eq. (12) yields directly the extent of crack closure at zero applied stress. Combination of Eqs. (5), (6) and (12) yields the crack closure stress S_{cc}. The stress Parameters τ_i, S, ΔS and the shear modulus μ in Eqs. (5) to (12) are made dimensionless by expressing these parameters in units of τ_i. These equations could not be solved analytically. The interesting parameters such as B, B_r, S_{cc}, S for given inputs of crack width (2a), slip band length (ℓ), friction stress (τ_i), slip plane angle (θ), and shear modulus (μ) can be readily obtained by numerical iteration. Typical plots of B, B_r, versus S/τ_i for aluminum alloys are shown in Figs. 2 and 3, respectively, for $\theta = 70°$ and 2a = 100, 150 microns. The corresponding solutions of ℓ, satisfying the singularity suppression Eq. (6) for the respective values of B and S/τ_i, are also shown in Figs. 2 and 3 as dotted curves.

In order to evolve the change of crack closure stress S_{cc}/S_{max} (normalized with respect to maximum applied stress S_{max}) with slip band length ℓ/a (normalized with respect to half crack width a) from the plots shown in Figs. 2 and 3, it is necessary to make some assumptions in regard to the change of friction stress τ_i with slip band dislocation density. The slip band thickness is assumed to increase in direct proportion to its width, so that for

a given superdislocation Burger's vector the average dislocation density is inversely proportional to the square root of the slip band length. If one further assumes that the friction stress to superdislocation motion is directly proportional to the slip band dislocation density [21], it follows

$$\tau_i/\tau_o = \sqrt{(B/\ell)_i/(B/\ell)_o} \tag{13}$$

where τ_o and $(B/\ell)_o$ are some arbitrarily chosen reference state corresponding to friction stress τ_o and slip band width ℓ_o. The crack closure stresses calculated according to Eq. (13) are plotted versus the ℓ/a values for $\theta = 70°$ as solid curve in Fig. 4. The results from finite element analyses (see next section) are also shown in Fig. 4 as a dotted curve. Experimental data [16] for a high strength aluminum alloy from our laboratory are presented in Fig. 4 as solid circles.

III. FINITE ELEMENT ANALYSES

The NASTRAN [22] cracked plate piecewise linear analysis program with triangular (CTRMEM) elements was used in this study. The cracked plate has two planes of symmetry, so only one quarter of the plate needs to be structured and analyzed. A schematic diagram of the elements representing one quarter of a cracked plate is shown in Fig. 5. The total number of nodal points and triangular elements used varies with the plate width (in the X-direction) to the crack width ratio studied. The right edge of the cracked plate is constrained

from moving in the X-direction to simulate a fixed boundary. The analysis involves stressing the plate in the Y-direction in increments and recalculating the material properties for each element as a function of the element stress for the last load increment. Plastic, rather than nonlinear elastic, behavior is assumed. The theoretical basis of two dimensional plastic deformation used in NASTRAN is that developed by Swedlow [23]. A typical uniaxial stress-strain curve for 7075-T6 aluminum alloy was used in the present investigation. Upon incremental loading to the maximum stress S_{max}, loading was decreased incrementally until the first contact of the cracked nodal point or points, at which the applied stress is called the crack closure stress S_{cc}. Results for S_{cc}/S_{max} are plotted versus ℓ/a values (where $\ell = w - a$, w being the half plate width, and a the half crack width) in Fig. 4 as dotted curves for comparison with the solid curves from Section II according to the superdislocation model. In the finite element analyses, S_{max} was chosen to be nine-tenth of the yield stress of the material in all the calculations.

IV. DISCUSSION

In Figures 2 and 3 the ratio of the applied stress to friction stress is plotted, regardless of the state of the friction stress. During cyclic stressing, the friction stress during the loading cycle may differ from that during the unloading cycle. The effect of variation of the friction stress τ_f, can thus be readily taken into consideration by the appropriate modification of the τ_f values. Although these calculations are based on a very simplified

superdislocation model, they do provide theoretical support of the existence of crack-closure phenomenon in fatigue crack growth under plane strain conditions. It should be noted in Figs. 2 and 3 that, for each data point of the superdislocation Burger's vector versus S/τ_f curve, there is a unique slip band width which satisfies the singularity suppression Eq. (6). The corresponding slip band width values are plotted versus S/τ_f also in Figs. 2 and 3 as dotted curves. The predicted dependence of crack closure on slip band width, based on a simplified friction stress model according to Eq. (13) (see Fig. 4), is in reasonably good agreement with the finite element analyses results described in Section III and with experimental observations [16].

ACKNOWLEDGEMENT

This work was supported in part by Contract No. N00014-79-C-0334 with the Office of Naval Research. The author wishes to thank W.L. Morris, Rockwell International Science Center, for helpful discussions.

REFERENCES

[1] W. Elber, "Fatigue Crack Closure Under Cyclic Tension," Engineering Fracture Mechanics 2, (1970) 37-45.

[2] W. Elber, "The Significance of Fatigue Crack Closure," Damage Tolerance in Aircraft Structures, ASTM STP 486, (1971) 230-242.

[3] T.C. Lindley and C.E. Richards, "The Relevance of Crack Closure to Fatigue Crack Propagation," Materials Science & Engineering 14, (1974) 281-293.

[4] J.C. Newman, Jr., "A Finite Element Analysis of Crack Closure," Mechanics of Crack Growth, ASTM STP 590, (1971), 281-301.

[5] K. Ohji, K. Ogura and Y. Ohkubo, "Cyclic Analysis of a Propagating Crack and Its Correlation with Fatigue Growth," Engineering Fracture Mechanics 7, (1975), 457-464.

[6] K. Ogura and K. Ohji, "FEM Analysis of Crack Closure and Delay Effect in Fatigue Crack Growth Under Variable Amplitude Loading," Engineering Fracture Mechanics, 9, (1977) 471-480.

[7] A. Otsuka, K. Mori and T. Miyata, "The Condition of Fatigue Crack Growth in Mixed Condition Mode," Engineering Fracture Mechanics, 7, (1975) 429-439.

[8] A.J. McEvily, "Current Asepcts of Fatigue," Metal Science, 4 (1977), 274-284.

[9] L.N. McCartney, "A Theoretical Explanation of the Delaying Effects of Overloads on Fatigue Crack Propagation," Internatinal Journal of Fracture 14, (1978), 213-232.

[10] B. Budiansky and J.W. Hutchinson, "Analysis of Closure in Fatigue Crack Growth," Journal of Applied Mechanics 45, (1978), 267-276.

[11] L.N. McCartney, "A Note on Closure During Fatigue Crack Growth," International Journal of Fracture 15, (1979), R21-24.

[12] C. Atkinson and M.F. Kanninen, "A Simple Representation of Crack Tip Plasticity: The Inclined Strip Yield Superdislocation Model," International Journal of Fracture 13, (1977), 151-163.

[13] M.F. Kanninen, C. Atkinson and C.E. Feddersen, "A Fatigue Crack Growth Analysis Method Based on a Simple Representation of Crack-Tip Plasticity," Cyclic Stress-Strain and Plastic Deformation Aspects of Fatigue Crack Growth, ASTM STP 637, (1976) 122-140.

[14] J.T. Evans, "Reverse Shear on Inclinded Planes at the Tip of a Sharp Crack," Journal Mechanics Physics of Solids 27 (1979) 73-88.

[15] J. Lindigkeit, G. Terlinde, A. Gysler and G. Lutjering, "The Effect of Grain Size on the Fatigue Crack Propagation Behavior of Age-Hardened Alloys in Inert and Corrosive Environment," Acta Metallurgica 17, (1979) 1717-1726.

[16] W.L. Morris, Accepted for publication in Metallurgical Transactions.

[17] B.A. Bilby and K.H. Swinden, "Representation of Plasticity at Notches by Linear Dislocation Arrays," Proceedings Royal Society A285, (1965) 22-33.

[18] V. Vitek, "Yielding on Inclinded Planes at the Tip of A Crack Loaded in Uniform Tension," Journal Mechanics Physics of Solids, 24, (1976) 263-275.

[19] H. Riedel, "Plastic Yielding on Inclinded Slip-Planes at a Crack Tip," Journal Mechanics Physics of Solids, 24, (1976) 277-289.

[20] N.I. Muskhelishvili, "Some Basic Problems of the Mathematical Theory of Elasticity," Translated from the Russian by J.R.M. Radok, 1963, Noordhoff, Groningen, The Netherlands, p.1.

[21] R. Chang, W.L. Morris and O. Buck, "Fatigue Crack Nucleation at Intermetallic Particles in Alloys," Scripta Metallurgica 13, (1979) 191-194.

[22] NASA Stress Analyses Program (NASTRAN) NASA SP-223(05), maintained and updated at Rockwell International.

[23] J. L. Swedlow, "The Thickness Effect and Plastic Flow in Cracked Plates," Aerospace Research Laboratories, Wright Patterson Air Force Base, Ohio, ARL 65-216, October 1965.

LIST OF FIGURES

SC80-8065

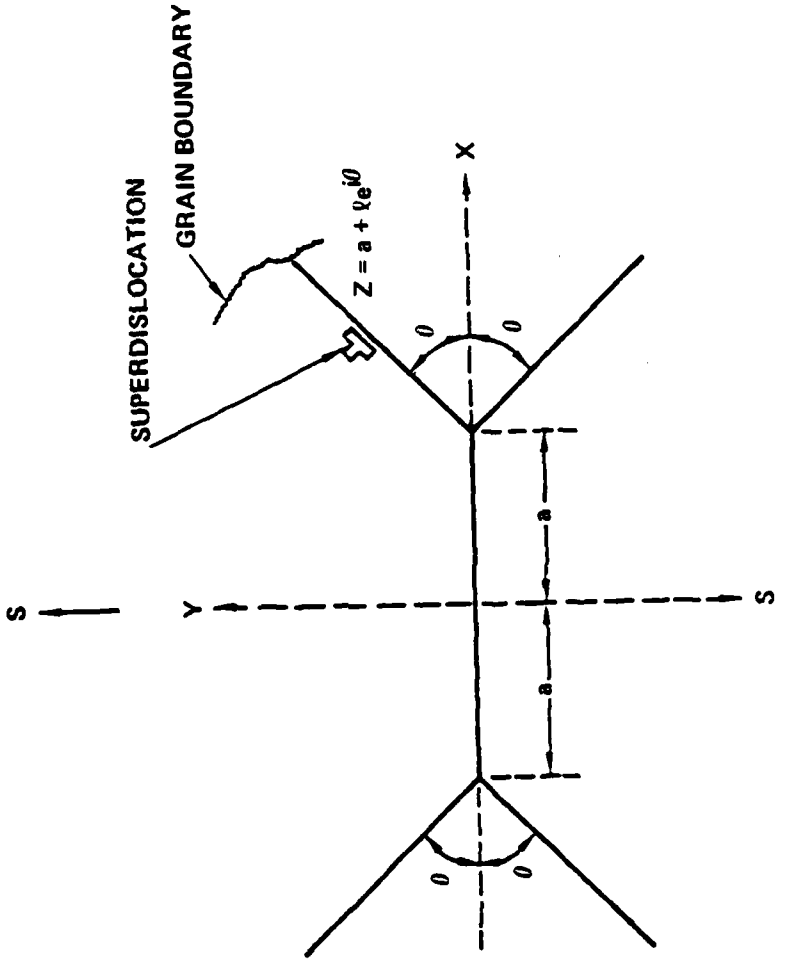

Fig. 1

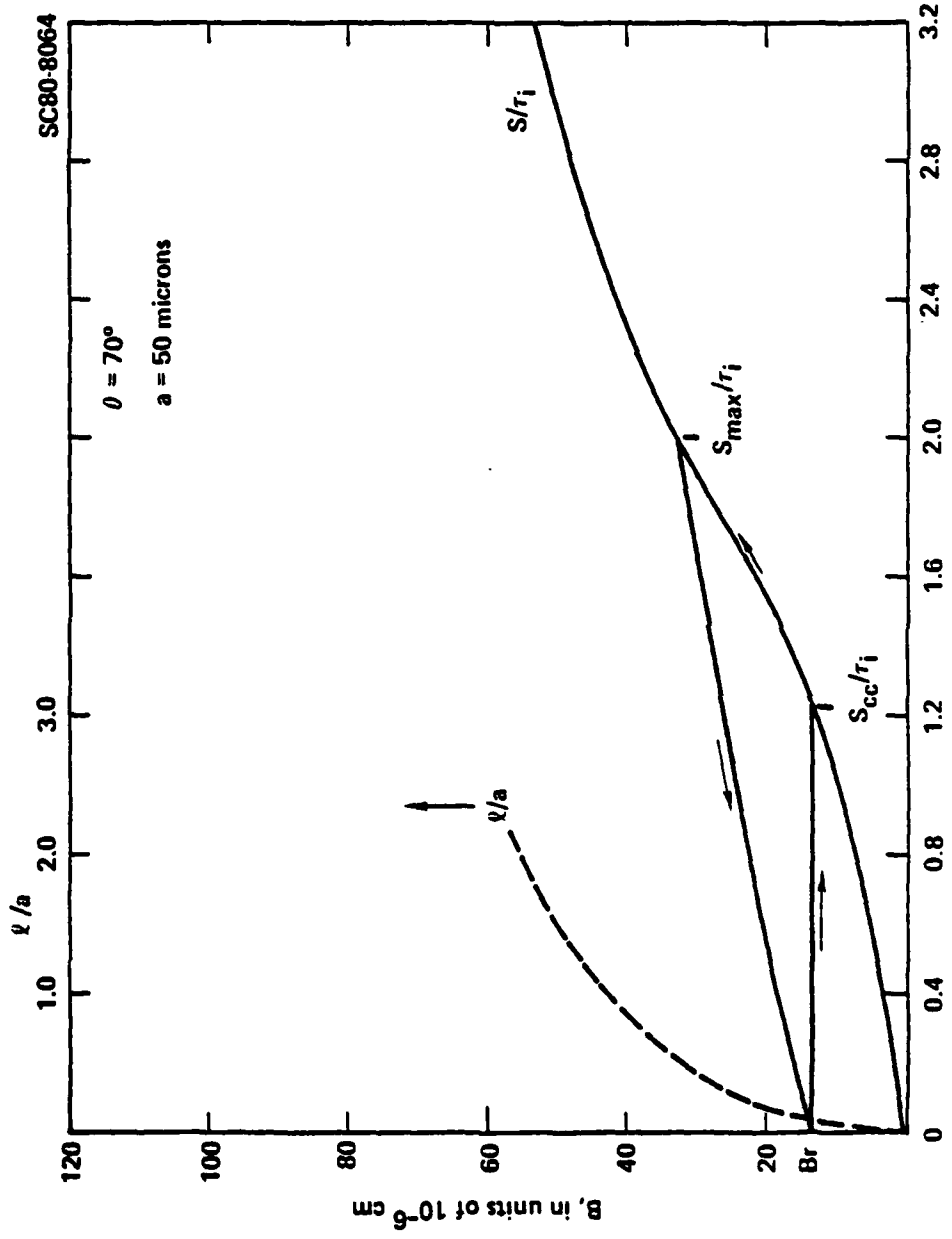
SC80-8064
θ = 70°
a = 50 microns
S/r_i
S_{max}/r_i
S_{cc}/r_i
ℓ/a
Br
B, in units of 10^{-6} cm
ℓ/a
S/r_i
120
100
80
60
40
20
0
1.0
2.0
3.0
0.4
0.8
1.2
1.6
2.0
2.4
2.8
3.2

Fig. 2

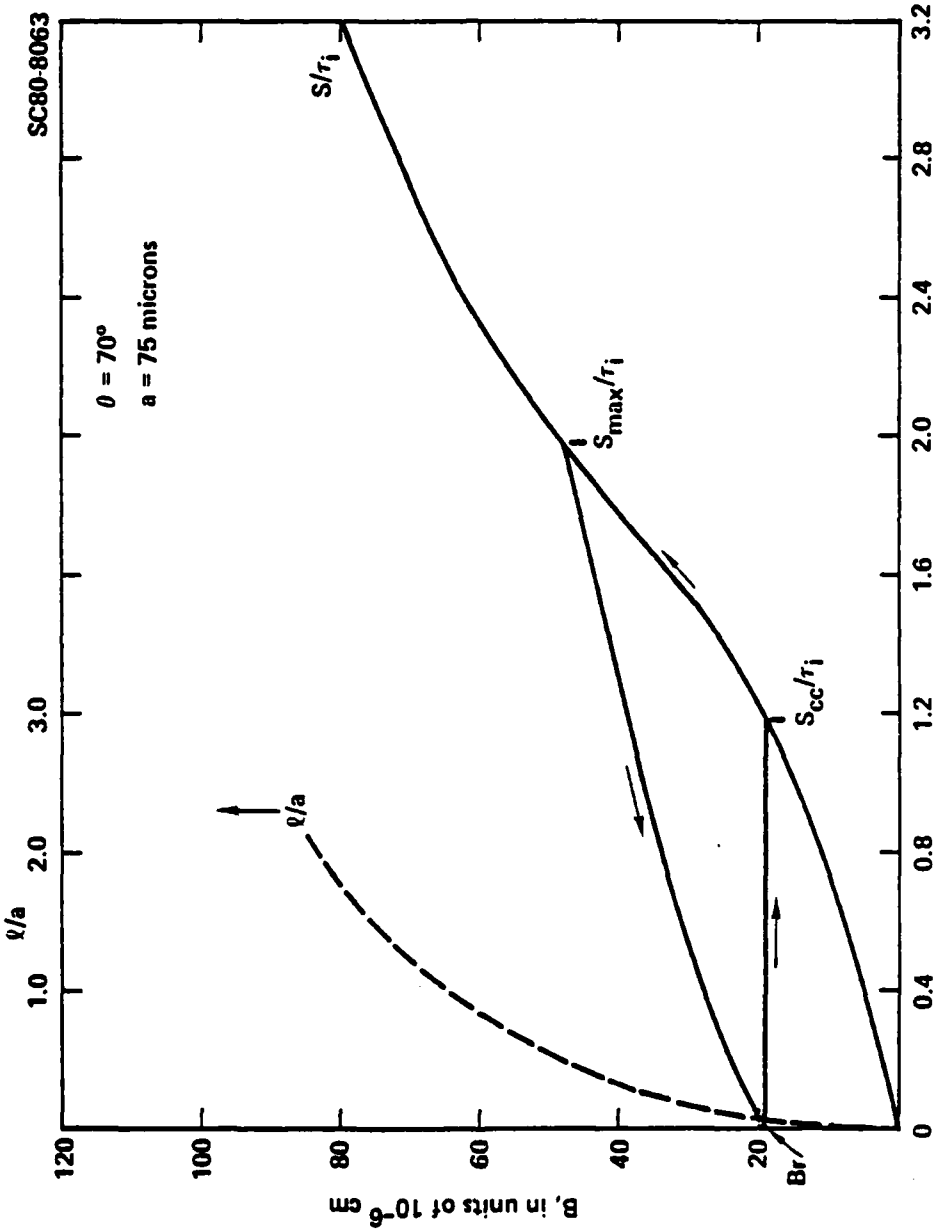
SC80-8063
θ = 70°
a = 75 microns
S/r_i
S_max/r_i
S_cc/r_i
ℓ/a
Br
B_r in units of 10^-6 cm
S/r_i
ℓ/a
120
100
80
60
40
20
0
0.4
0.8
1.2
1.6
2.0
2.4
2.8
3.2
1.0
2.0
3.0

Fig. 3

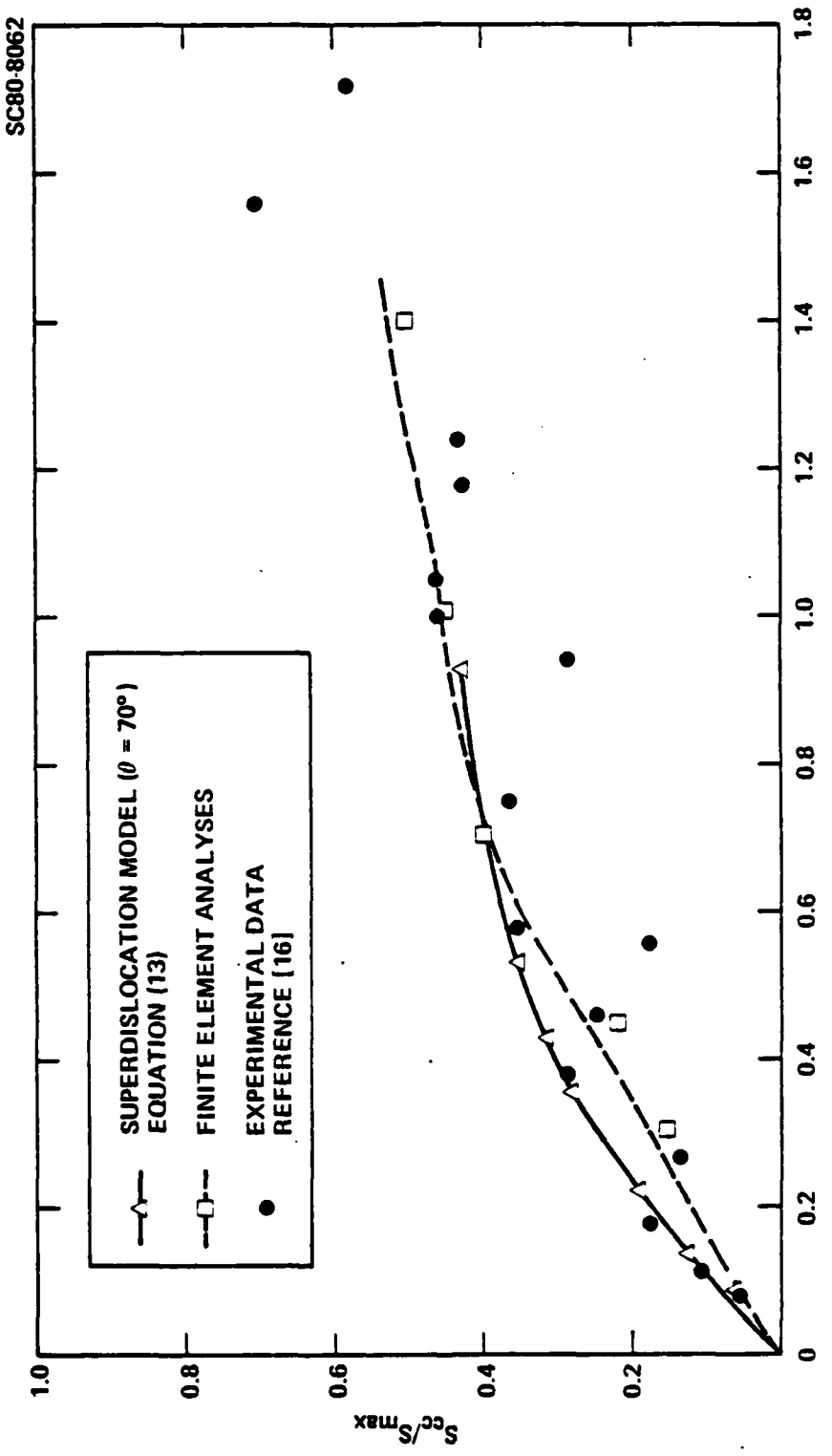
SC80-8062
SUPERDISLOCATION MODEL (θ = 70°)
EQUATION (13)
FINITE ELEMENT ANALYSES
EXPERIMENTAL DATA
REFERENCE [16]
S_{cc}/S_{max}
ℓ/a
0
0.2
0.4
0.6
0.8
1.0
1.2
1.4
1.6
1.8

Fig. 4

SC80-8061

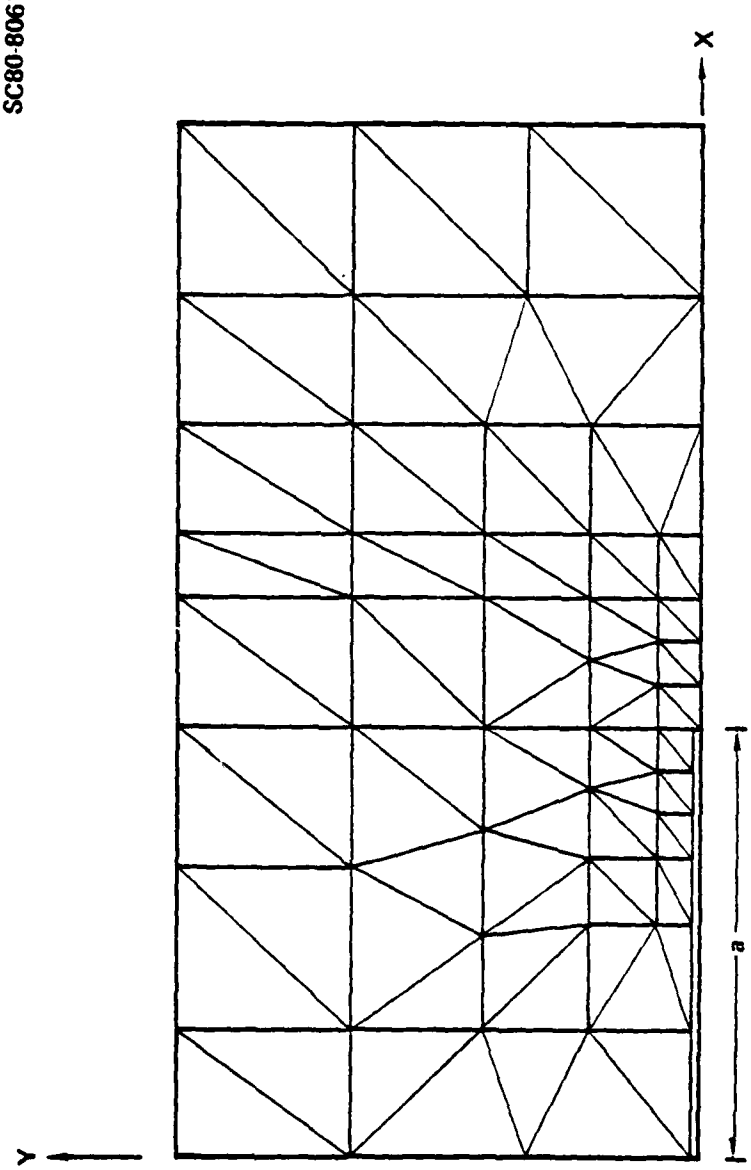

Fig. 5